universität wien

MASTERARBEIT / MASTER'S THESIS

Titel der Masterarbeit / Title of the Master's Thesis

„Coronaridine congener interaction with $\alpha_3\beta_4$, $\alpha_3\beta_4\beta_2$ and $\alpha_3\beta_4\alpha_5$ nicotinic acetylcholine receptors in neurons of the native mouse superior cervical ganglion“

verfasst von / submitted by

Thomas Ackerbauer, BSc

angestrebter akademischer Grad / in partial fulfilment of the requirements for the degree of

Master of Science (MSc)

Wien, 2021 / Vienna, 2021

Studienkennzahl lt. Studienblatt / degree programme code as it appears on the student record sheet:	A 066 834
Studienrichtung lt. Studienblatt / degree programme as it appears on the student record sheet:	Masterstudium Molekulare Biologie UG2002
Betreut von / Supervisor:	Assoc. Prof. Priv. Doz. Mag. Dr. Petra Scholze

Declaration

This thesis project was realized at the Center for Brain Research, Medical University of Vienna. The study concept was prepared by Assoc. Prof. Priv. Doz. Mag. Dr. Petra Scholze, and Thomas Ackerbauer, BSc. Breeding and dissection of all mice were conducted by Assoc. Prof. Priv. Doz. Mag. Dr. Petra Scholze.

All other experiments, data analysis and interpretation were performed by Thomas Ackerbauer under supervision of Assoc. Prof. Priv. Doz. Mag. Dr. Petra Scholze and Prof. Dr. Sigismund Huck at the Department of Pathobiology of the Nervous System within the Center for Brain Research.

I have tried to locate all copyright holders and obtain their consent to use the images in this work. Should nevertheless a copyright infringement become known, please contact me.

Acknowledgement

I first want to thank Petra Scholze for the opportunity to work in her lab and realize this Master thesis and her great support during the experimental time. I also want to thank Sigismund Huck who guided me during the time I worked in the lab especially the electrophysiological experiments and always had an open ear for my questions.

My sincere thanks also go to Friederike Steudle and Xenia Simeone who were always helpful when I had a question or problem and as well Hugo Arias who gifted us the substances which made this project feasible.

Last but not least I want to thank my family and my girlfriend Ivana for all their love and great motivational support.

Table of Contents

1 Abstract

Nicotinic acetylcholine receptors (nAChRs) have gained broad attention over the past decades for their interactive role in the brains reward system. This is especially true for $\alpha_3\beta_4$ containing receptors, which are highly expressed in neurons of the medial habenula and the interpeduncular nucleus, mediating withdrawal symptoms. Several previous studies suggested that the two coronaridine congeners (+)–catharanthine and 18-Methoxycoronaridine (18-MC) could be promising novel drug candidates, since they showed to be non-competitive inhibitors of $\alpha_3\beta_4$, $\alpha_3\beta_4\beta_2$ and $\alpha_3\beta_4\alpha_5$ containing nAChRs. However, until today those compounds have only been investigated in heterologous expression systems. In the current study I now aim to investigate the interaction of coronaridine congeners with native $\alpha_3\beta_4$ containing receptors.

I conducted electrophysiological measurements on cultured primary neurons of the mouse superior cervical ganglion (SCG) containing distinct $\alpha_3\beta_4$ nAChRs. I used wild type (WT) mice, expressing $\alpha_3\beta_4$, $\alpha_3\beta_4\beta_2$ and $\alpha_3\beta_4\alpha_5$ nAChRs and α_5 or β_2 knockout (KO) mice, expressing $\alpha_3\beta_4$, $\alpha_3\beta_4\beta_2$ or $\alpha_3\beta_4$ and $\alpha_3\beta_4\alpha_5$ nAChRs as well as double KO ($\alpha_5\beta_2$ KO) mice, expressing only $\alpha_3\beta_4$ nAChRs.

My results showed that the two congeners rapidly and reversibly inhibited (±)-epibatidine induced currents in all of the different receptor subunits.

I found differences of the inhibition potencies not only between the two congeners but also between the different receptor subtypes expressed in WT and KO neurons. My findings suggest that nicotinic $\alpha_3\beta_4$ containing receptors differ in their properties towards the investigated coronaridine congeners depending on the presence or absence of the α_5 and β_2 accessory subunit.

2 Introduction

Nicotinic acetylcholine receptors (nAChRs) are large glycoprotein- (~290 kDa), ligand gated ion channels activated by the endogenous neurotransmitter acetylcholine (ACh) which evokes rapid excitatory responses in matter of milliseconds.

About 50 years ago, nAChRs were the first neurotransmitter receptors to be isolated and purified from the electric organs of *Torpedo californica* ray, which finally made it possible to study and characterize receptor structure and function in depth. In the following years it turned out, that they are members of a superfamily of Cys-loop ligand gated ion channel receptors together with the muscle and the neuronal type nAChRs, GABA type A, GABA type C, glycine and 5-HT_3 receptors. Cys-loop receptors play prominent roles in generating excitatory and inhibitory postsynaptic potentials in the nervous system. nAChRs can be found in the central (CNS) - and the peripheral nervous system (PNS) as well as non-neuronal tissues. The receptors respond not only to ACh, but to several different agonists like e.g. their eponym nicotine (Albuquerque *et al.*, 2009; Gahring and Rogers, 2006; Gotti *et al.*, 2009), but also the alkaloid plant toxin cytisine, the frog-toxin epibatidine, and many more (Gotti *et al.*, 2006).

In the mammalian CNS, nAChRs can be found in cortical as well as in many subcortical structures like the striatum, hippocampus or thalamic - and monoamine nuclei which modulate cortical processes (Wilens and Decker, 2007). They are either expressed in neurons or non-neuronal cells like microglia, astrocytes and oligodendrocyte precursor cells as well as endothelial cells where they are found to be involved to the neural immune system and neuroprotection (Dineley *et al.*, 2015).

The fast ionotropic receptors play an essential role in transganglionic signal transmission and cognitive processes, are associated with diverse physiological functions like processing of pain, anxiety, sleep, and motor-activity at the neuro-muscular endplate and are also participating in different pathological conditions like schizophrenia, Alzheimer's - or Parkinson's disease (Gotti *et al.*, 2006; Wang *et al.*, 2003). In addition there are findings that nAChRs which are located in the habenulo-interpeduncular cholinergic pathway (HICP) are thought to be associated with drug withdrawal and drug dependence e.g. nicotine abuse (McCallum *et al.*, 2012).

nAChRs are attractive targets for drugs against psychiatric and neurodegenerative disorders as well as anti-addictive agents and cessation aids against withdrawal symptoms caused by substances such as nicotine, cocaine, morphine and others.

In the past decades two substances have attracted very strong interest because of their anti-addictive properties on nAChRs. The two coronaridine congeners, (+)–catharanthine and 18-MC are found to reduce drug self-administration in animals as well as withdrawal effects in

humans and are known non-competitive antagonists (NCAs) of several nAChRs especially $\alpha_3\beta_4$ subunit containing receptors that are highly expressed in the HICP (Arias *et al.*, 2017). Those compounds have so far only been investigated in heterologous expression systems. The purpose of this work is to investigate the interaction of coronaridine congeners with native $\alpha_3\beta_4$ containing receptors in cultured primary neurons and participate on the development of novel analogs for safer anti-addictive therapies.

2.1 Nicotinic acetylcholine receptors

2.1.1 Structure of the nAChR

nAChRs are pentameric structures formed by a compilation of five out of 17 individual subunits (α_1-α_{10}, β_1-β_4, γ-, δ- and ε) which are differently expressed throughout the nervous system. The receptors are generally subdivided into muscle and neuronal type receptors, each of them building up a specific subunit arrangement (Hogg *et al.*, 2003).
Muscle type nicotinic acetylcholine receptors (mnAChRs) which are located at the skeletal neuromuscular junctions include the α_1, β_1 γ-, δ- and in adults the ε−subunits and are responsible for the motor nerve-muscle-communications which lead to voluntary and involuntary contractions, whereas in neuronal type nAChRs the subunits $\alpha_2 – \alpha_{10}$ and $\beta_2 – \beta_4$ can be found (Albuquerque *et al.*, 2009).

Integrated into the cell - or postsynaptic-membrane each of the subunits consists of four transmembrane spanning α-helical domains M1, M2, M3 and M4, with a large extracellular domain, beginning from the hydrophilic amino-terminus (-NH2) and merging into the transmembrane M1 domain. Two intracellular domains (loops) connect either M1 and M2 or M3 and M4 and an extracellular domain connects M2 and M3. A short extracellular domain that connects to M4 ends with the carboxy-terminus (-COOH) (Figure 1, B) (Albuquerque *et al.*, 2009; Corringer *et al.*, 2000).
The four transmembrane domains (M1 – M4) are organized in concentric layers around the water filled ion pore where the M2 domains from each of the five subunits build the major part of the inner pore surrounded by M1, M3 and M4 to shield them from the surrounding lipid bilayer (Figure 1). The water filled ion pore is responsible for the controlled flow of specific small monovalent or divalent ions over the cellular membrane and its structure is different depending on the receptors activation state (open, closed or desensitized).
The N-terminal domain that emerges into M1 holds the Cys-loop which is characterizing for the superfamily of Cys-loop receptors. The Cys-loop is built by two disulfide linked cystines which are separated by 13 highly conserved amino acids. Also characteristic is a Cys-Cys

pair at the N-terminal extracellular domain which is required by α-subunits (α_1, α_2, α_3, α_4, α_6, α_7, or α_9) to form the front side of the hydrophobic ligand binding pocket with adjacent subunits. The α_{10}, β_2, β_4, δ, γ, or ε, as adjacent subunits participate to the back side of the binding pocket (Albuquerque *et al.*, 2009).

The much bigger intracellular loop that connects M3 and M4 is involved in subunit assembly and the targeting, clustering and anchoring of the assembled receptors in the cellular membrane (Borges and Ferns, 2001; Dani and Bertrand, 2007; Gotti *et al.*, 2009). The domains differ between the several subunits which lead to a variability in their properties due to intracellular modifications, cytoskeletal connections as well as surface distribution. Each subunit can as well be glycosylated at one or more of their extracellular domains (Corringer *et al.*, 2000; Kracun *et al.*, 2008).

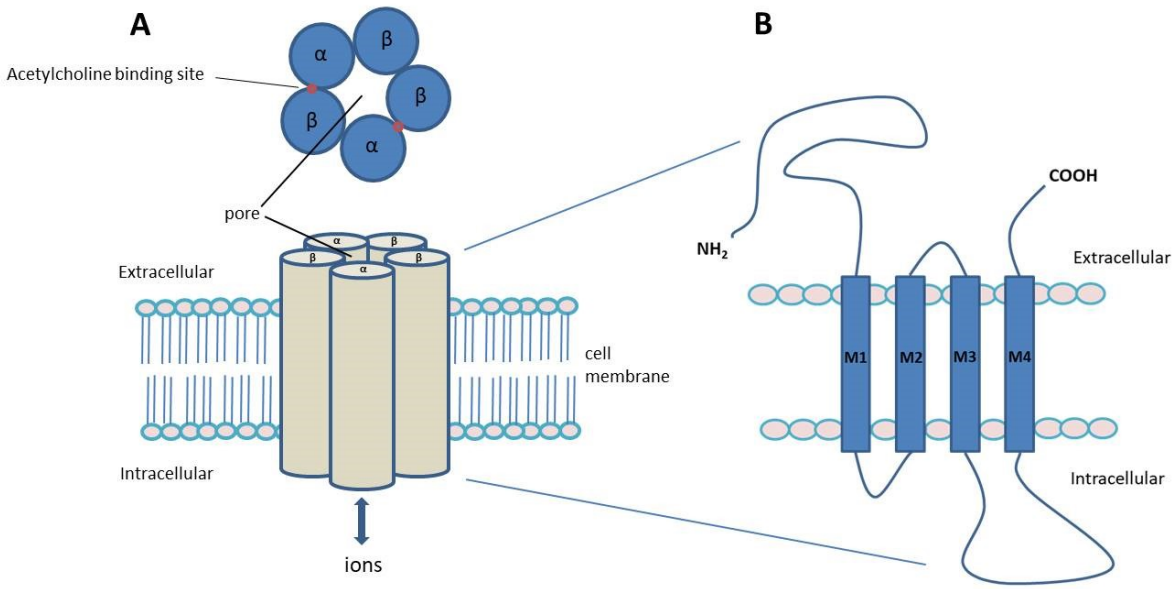

Figure 1 - Schematic representation of a nAChR, its subunits and the intra- extracellular- and membrane spanning domains

(A) nAChR receptor with 2 α and 3 β subunits spanning through the cell membrane. The circular arrangement of the subunits forms the ion pore through the membrane. Acetylcholine binding sites are indicated by the red dots between the α and β subunits. **(B)** Each subunit consists of four transmembrane spanning domains M1-M4 which are connected by either an intra- or extracellular loop. At the extracellular site a long amino terminal domain (-NH_2) emerges into the domain M1 and a short carboxy terminal domain (-COOH) emerges from the transmembane domain M4.

2.1.2 Accessory subunits of nAChRs

Accessory subunits like the α_5, embedded in a e.g. $2(\alpha_4)2(\beta_2)(\alpha_5)$ receptor and the β_3-subunit do not directly contribute to the agonist binding sites, they play their role in a way of modifying the functional properties of the receptor. The presence of α_5 subunits increases the rate of desensitization and the calcium permeability of receptors containing $\alpha_3\beta_2$ or $\alpha_3\beta_4$ subunits, but it is not able to build functional receptors neither alone nor with any other β-subunits when expressed in a heterologous expression system (Gerzanich *et al.*, 1998; Ramirez-Latorre *et al.*, 1996).

In addition to α_5 and β_3 the subunits α_3, α_4, β_2 and β_4 are able to build functional receptors and contribute to the agonist binding site but they are as well able to be located in the accessory subunit position and thus can change the receptors pharmacological and biophysical properties as well as their sensitivity to agonists, antagonists, modulators and their permeability for ions (Dani, 2015; Fasoli and Gotti, 2015; Gotti *et al.*, 2009).

2.1.3 Homo- and hetero-oligomeric receptors

Subunits of nAChRs can form either homo- or hetero-oligomers. Hetero-oligomeric receptors are built by a combination of distinct α or β receptor subunits where homo-oligomeric receptors have been shown to be formed by only one type of either α_7, α_8 or α_9 subunits alone (Figure 2).

In hetero-oligomeric receptors, the ligand binding sites are found between the α- and β– or α- and α-subunits. In the homo-oligomeric variant each of the five α subunits builds an agonist binding site with its adjacent subunits (Albuquerque *et al.*, 2009).

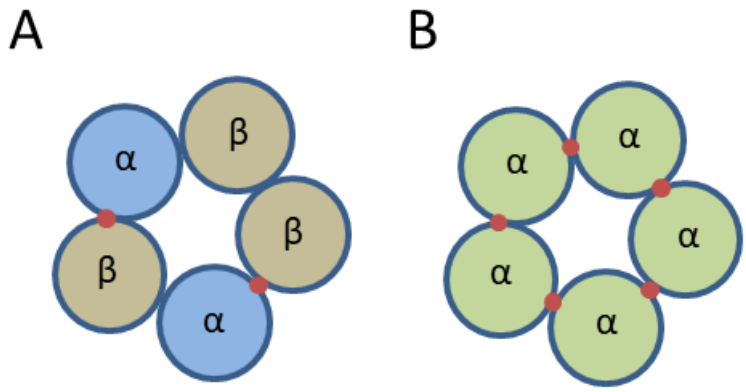

Figure 2 - Schematic illustration of the nAChRs subunit arrangement

nAChR consist of an arrangement of five out of a huge variety of different subunits. Here shown the **(A)** Typical hetero-oligomeric receptor with 2 α-and 3 β-subunits, the **(B)** homo-oligomeric receptor that can be formed by either α_7, α_8 or α_9 – subunits.

2.1.4 nAChR subunit expression and arrangements

Depending on the location being expressed and their functional roles, nAChRs show a huge variation of different subunit assemblies. The International Union of Basic and Clinical Pharmacology Committee on Receptor Nomenclature and Drug Classification (NC-IUPHAR, URL: http://www.guidetopharmacology.org/nciuphar.jsp) recommends a nomenclature and classification scheme for nAChRs based on subunit arrangement of known, naturally occurring or heterologous-expressed nAChR subunits (Table1). A total of 17 subunits (α_1–α_{10}, β_1– β_4, γ, δ, and ε) have been identified in nAChRs whereas the α_8 subunits have not been found in mammals yet, but are expressed in avian species such as e.g. chicken (Keyser *et al.*, 1993).

mnAChRs can only assemble in the following two combinations: embryonic mnAChRs $2(\alpha_1)(\beta_1)(\gamma)(\delta)$ and adult mnAChRs $2(\alpha_1)(\beta_1)(\delta)(\varepsilon)$ (Figure 3) (Albuquerque *et al.*, 2009).

Neuronal nAChRs can assemble as homo- or hetero-oligomers and are generally found in the two stoichiometries 2(α)3(β) and 3(α)2(β). The predominant nAChRs in the CNS contain the two stoichiometries $2(\alpha_4)3(\beta_2)$ and $3(\alpha_4)2(\beta_2)$ but even compositions out of three or four different subunit types have been identified e.g. $2(\alpha_4)2(\beta_2)(\alpha_5)$ (David *et al.*, 2010; Hogg *et al.*, 2003; Lloyd and Williams, 2000).

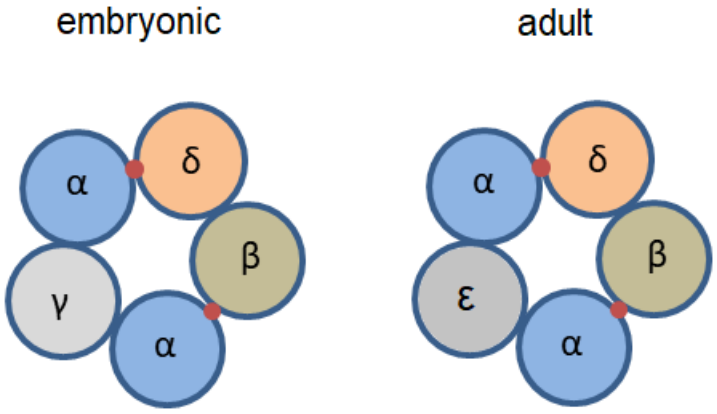

Figure 3 - Schematic illustration of the mnAChRs subunit arrangement

Embryonic and **adult** muscle type receptors including the α_1-, β_1-, γ-, δ-and ε subunits. The red dots indicate the ligand binding pockets.

In the mammal brain e.g. not only α_4 and β_2 subunits are found, many other combinations are possible in the distinct locations of the CNS and PNS. In e.g. the Interpeduncular nucleus (IPN), part of the central relay station between forebrain and midbrain the habenulo-interpeduncular complex (Hb-IPN), which is known for inhibitory effects on several other

brain regions, combinations of $\alpha_3\beta_4$, $\alpha_3\beta_3\beta_4$, $\alpha_3\beta_2$, $\alpha_2\beta_2$ and $\alpha_4\beta_4$ receptors have been found (Beiranvand *et al.*, 2014; Gotti *et al.*, 2009). Similarly in Habenula, combinations of $\alpha_3\beta_4$, $\alpha_3\beta_2$, $\alpha_4\beta_2$, $\alpha_3\beta_4\beta_2$, $\alpha_3\beta_4\alpha_4$, and $\alpha_3\beta_4\alpha_5\beta_2$ could be identified (Scholze *et al.*, 2012).
The α_7 receptor was found to play an important role in anti-inflammatory and neuroprotective processes when expressed in immune- and glial cells (Akaike *et al.*, 2018).
The most common receptor type in the PNS in turn consists of two α_3 and three β_4 subunits ($2(\alpha_3)3(\beta_4)$) but it is also possible to assemble in a $3(\alpha_3)2(\beta_4)$ way (Figure 4) (Krashia *et al.*, 2010).

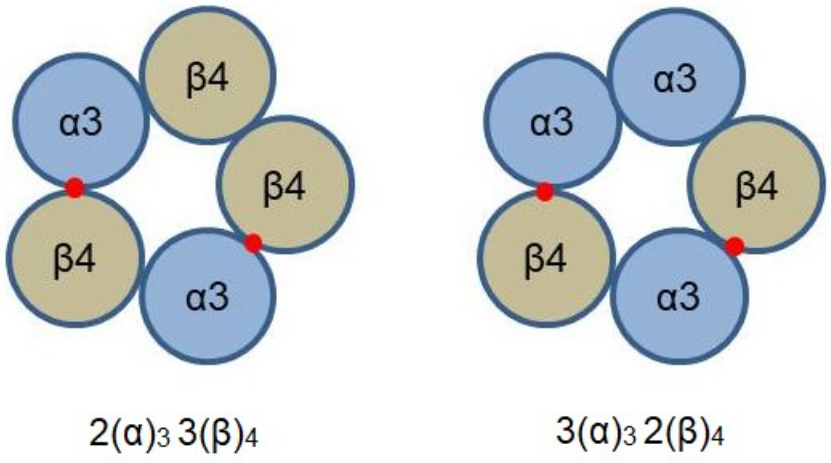

Figure 4 - Schematic representation of the two possible $\alpha_3\beta_4$ subunit arrangements

The most abundant nAChRs of the mammal PNS can arrange in two different stoichiometries $2(\alpha_3)3(\beta_4)$ and $3(\alpha_3)2(\beta_4)$. The red dots indicate agonist binding sites.

The mouse SCG as a part of its sympathetic nervous system contains neurons that supply innervation to many organs, glands and parts of the carotid system in the head. It maintains synaptic transmission and receives synaptic input from preganglionic axons (Fischer *et al.*, 2005). Four different receptor types are assembled in neurons of the adult WT mouse SCG, built by a compilation of the subunits α_3, α_5, α_7, β_2 and β_4. The α_3 subunit is essential in forming hetero-oligomeric nAChRs, and a KO would abolish synaptic transmission and lead to death (Rassadi *et al.*, 2005; Xu *et al.*, 1999).
In neurons of the adult WT mouse SCG, 100% of the hetero-oligomeric receptors contain the α_3 and β_4 subunits. About 55% of the receptors contain the α_3 and β_4 subunits alone, 24% also contain α_5, and 21% additionally hold β_2 (Figure 5) (David *et al.*, 2010). The α_5 subunit does not co-assemble with β_2 in the same receptor which leads to four possible receptor combinations: $\alpha_3\beta_4$, $\alpha_3\beta_4\alpha_5$, $\alpha_3\beta_4\beta_2$ and α_7. The α_7 subunits are only found in homo-oligomeric

receptors in the mouse SCG and do not co-assemble with other subunit types (David *et al.*, 2010).

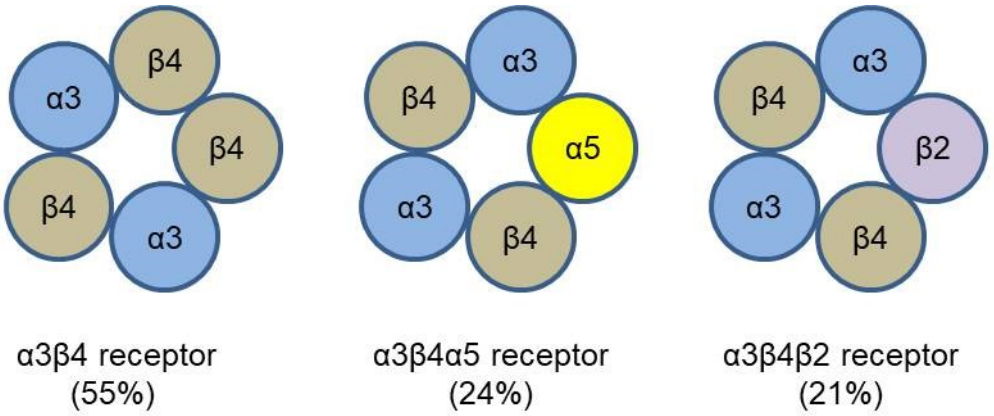

Figure 5 - Schematic representation of receptors expressed in neurons of the adult WT mice SCG

Excluding the homo-oligomierc α_7 –receptor, 100 % of the receptors in neurons of the SCG of adult WT mice contain the α_3 subunit. 55% of this are built up by $\alpha_3\beta_4$ alone, 24% include the α_5 subunit and about 21% include the β_2-subunit.

Table 1 - Stoichiometries and location of the most prominent different α-subunits of nAChRs

Subunit	Receptor subunit composition	Location	Species
α_1	Embryonic $2(\alpha_1)(\beta_1)(\gamma)(\delta)$ Adult $2(\alpha_1)(\beta_1)(\gamma)(\varepsilon)$	Neuromuscular junction	Mammals
α_2	$\alpha_2\beta_2$, $\alpha_2\beta_4$	CNS	Mammals
α_3	$\alpha_3\beta_2$, $\alpha_3\beta_4$	PNS (e.g. SCG), CNS (Habenula, IPN)	Mammals
α_4	$3(\alpha_4)2(\beta_2)$ $2(\alpha_4)3(\beta_2)$	CNS	Mammals
α_5	$\alpha_3\beta_2\alpha_5$, $\alpha_3\beta_4\alpha_5$, $2(\alpha_4)2(\beta_2)(\alpha_5)$	PNS (e.g. SCG), CNS (Habenula, IPN)	Mammals
α_6	$\alpha_6\beta_2\beta_3$, $\alpha_6\alpha_4\beta_2\beta_3$	CNS	Mammals
α_7	$5(\alpha_7)$	CNS, Non-neuronal cells	Mammals
α_8	$5(\alpha_8)$	CNS, Retina	Avian (e.g. Chicken)
α_9	$5(\alpha_9)$, $\alpha_9\alpha_{10}$	Mechanosensory hair cells	Mammals
α_{10}	$\alpha_9\alpha_{10}$	Mechanosensory hair cells	Mammals

2.1.5 Functional properties of nAChRs

Electrochemical signal transduction is the key function of the communication between pre- and postsynaptic nervous cells not only inside the nervous system itself, but also to communicate with other tissues like e.g. muscle cells or the endocrine system. If an action potential reaches the nerve terminal, voltage activated Ca^{2+} channels open and lead to an influx of Ca^{2+}. This in turn leads to the exocytosis of vesicles containing the nAChR agonist ACh into the synaptic gap. ACh diffuses across the synaptic cleft where it binds to nAChRs on the postsynaptic cell membrane (Figure 6) (Hammond, 2015).

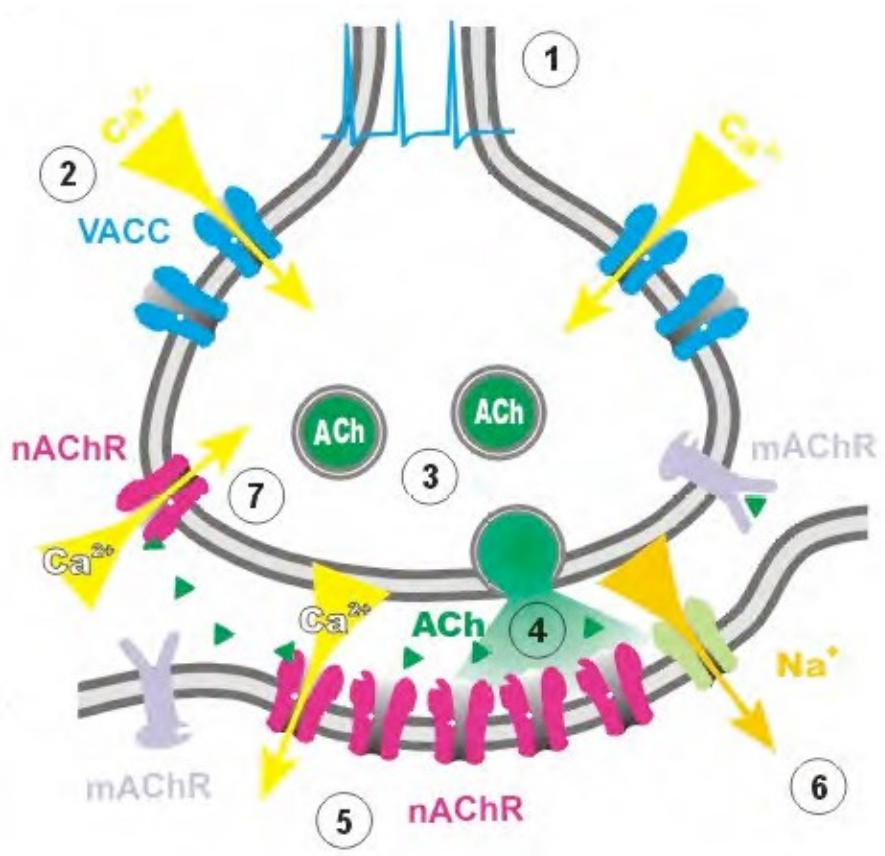

Figure 6 - Schematic representation of signal transmission between pre- and postganglionic nervous cells

(1) An action potential reaches the axonal endplate at the synaptic gap. **(2)** Voltage gated Ca^{2+} ion channels open and allow an influx of Ca^{2+} inside the cell. **(3)** Ca^{2+} influx leads to exocytosis of ACh filled vesicles at the presynaptic membrane where **(4)** ACh is released into the synaptic cleft and activates postsynaptic nAChRs. **(4) (5) (6)** The opening of the receptors forces an influx of positively charged ions that can lead to a further depolarization of the membrane and signal transduction. Adapted from (Fischer, 2003).

Opening and closing of nAChRs allows controlled flow of ions over the cellular membrane which can lead to different cellular responses of e.g. the postsynaptic cells or muscle cells. The receptors are very ion selective, which means they are only permeable to specific small

monovalent and divalent cations that can fit through the ion pore. Binding of nAChR agonists like ACh, nicotine or epibatidine to the hydrophobic binding pocket leads to a conformational change of the corresponding amino acids and a rotation of the transmembrane spanning domain M2 which in turn opens the hydrophilic ion channel in microseconds that allows an influx of positively charged ions like Na^+, K^+ and Ca^2 (Albuquerque *et al.*, 2009; Hama and Menzaghi, 2001).

This open conformation, also called the open state, is stabilized for several milliseconds by the binding of nAChR agonists and increases the permeability of the cellular membrane for ions rapidly. For this channel activation two molecules of agonist are required which have to be bound to each of the α-subunit ligand binding pockets. The agonist binding and the subsequent channel opening work due to positive cooperativity. This means that after the binding of the first agonist molecule to one α-subunit, the receptor undergoes a conformational change which enhances the probability and affinity of a second agonist molecule to bind (Arias, 2000). After ACh bound and opened the receptor, it is normally rapidly cleaved by the enzyme acetylcholine esterase into choline and acetic acid and choline is removed from the synaptic cleft by the choline transporter (ChT) and the receptor returns to the resting state (Karlin, 2009).

In the resting state conformation, the receptor is closed, has low affinity for a given agonist and is impermeable to ions. In addition to the opened and closed state, the receptors can also take in a so called “desensitized condition” caused by exposure to high concentrations of agonist, which can either be the fast onset desensitized state or the slow onset desensitized state. In both cases, the receptors are impermeable to ion flux through the cell membrane and the recovery from desensitization can take seconds to minutes. Desensitization is thought to control the use dependency of receptor agonists and can thus play a role in shaping synaptic efficacy and protecting cells from uncontrolled excitation (Fenster *et al.*, 1997; Hammond, 2015). In principle transitions from all of the four observed states into one another are possible (Figure 7) (Graupner and Gutkin, 2009).

The stoichiometry of the receptor and the number of different subunits can lead to different ligand binding sites and as well to different opening, closing and desensitizing kinetic properties. The $2(\alpha_4)3(\beta_2)$ receptor has other agonist binding sites and as a result of this different properties than e.g. the $3(\alpha_4)2(\beta_2)$ receptor. The $3(\alpha_4)2(\beta_2)$ nAChR contains two distinct agonist binding sites the $\alpha_4\beta_2$- and at the $\alpha_4\alpha_4$-interface where binding of the endogenous agonist ACh shows a biphasic activation response. This is not observed in $2(\alpha_4)3(\beta_2)$ nAChR´s which only contain the $\alpha_4\beta_2$-interface and binding of ACh shows a monophasic activation response (Harpsoe *et al.*, 2011). A mixture of both species Changes in the ratio of α_4 : β_2 strongly alters agonist sensitivity. This small change therefore can then

lead to completely different physiological properties of the receptor (Indurthi *et al.*, 2016; Krashia *et al.*, 2010; Son *et al.*, 2009; Tapia *et al.*, 2007).

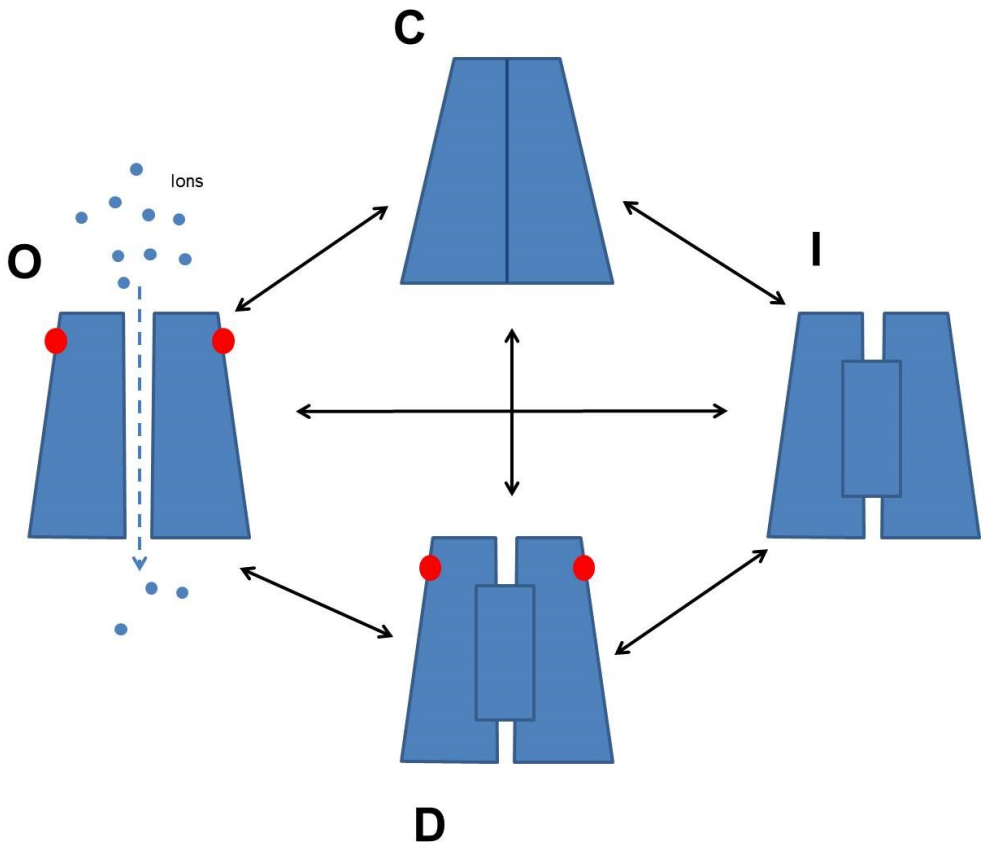

Figure 7 - Schematic illustrations of the possible conformational states of nAChRs

Possible conformational states of nAChRs **(O)** the open state is caused by agonist binding (red dots) and leads to an opening of the ion pore which allows ions to pass through the cell membrane. **(C)** The closed state is caused by an absence of agonist; no ion flux through the receptor is possible. **(D)** Indicates the desensitized state which is caused by an exposure of high agonist concentrations. Agonist can be still bound to the inactivated receptor. **(I)** inactivated desensitized state, no agonist is bound to the receptor and it cannot be activated.

Research up to date showed that the subunit assembly which is highly regulated in vivo can be easily manipulated in heterologous expression systems by e.g. transfection of different amounts of cDNA force the receptor stoichiometry ratio in a desired direction or the use of different host organisms with their own specific environment or longtime exposure to nicotine. Changings in the ratio of α and β subunits not only affects the agonist sensitivity, the different stoichiometries also show alterations in Ca^{2+} permeability (Harpsoe *et al.*, 2011; Indurthi *et al.*, 2016; Krashia *et al.*, 2010; Son *et al.*, 2009; Tapia *et al.*, 2007).

There are a huge number of different possible subunit arrangements to build a functional receptor. Each of them has individual functional and structural properties, which also make them more or less affine to different nAChR ligands. E.g. nAChRs which contain α_7 subunits

bind α-bungarotoxin, a nAChR antagonist neurotoxin from the venom of elapid snakes, they show low affinity to nicotine and have fast kinetics. In contrast β_2-containing receptors show a high affinity for nicotine and relatively slow kinetics; they do not bind α-bungarotoxin and desensitize to low agonist concentrations (Dani, 2015; Fasoli and Gotti, 2015).

2.1.6 Agonists of nAChRs

nAChR agonists bind to the same receptor binding pocket as ACh and favor the conformational changes of the protein towards the open state, which allows an influx of ions into the cell. Examples of the probably best-known agonists of nAChRs are the endogenous neurotransmitter ACh, nicotine, which gave the receptors their name, (+)-epibatidine, (-)-cytisine, the synthetically produced 3,4-Dimethylpyrazole phosphate (DMPP) and many others (Figure 8). They all activate the receptors with different potencies and are more or less specific for distinct receptor subunit assemblies (David *et al.*, 2010; Yost and Winegar, 1997).

ACh the endogenous neurotransmitter is synthesized in axon terminals from choline and acetyl coenzyme A (acetyl-CoA) and stored in vesicles at the end of cholinergic neurons. It will be rapidly released into the synaptic cleft upon nerve excitation and interacts with its target receptors on post synaptic cells. Subsequently after its transmission ACh is cleaved by the enzyme acetylcholine esterase into choline and acetic acid and choline is removed from the synaptic cleft by the ChT within a few milliseconds (Akaike *et al.*, 2018).

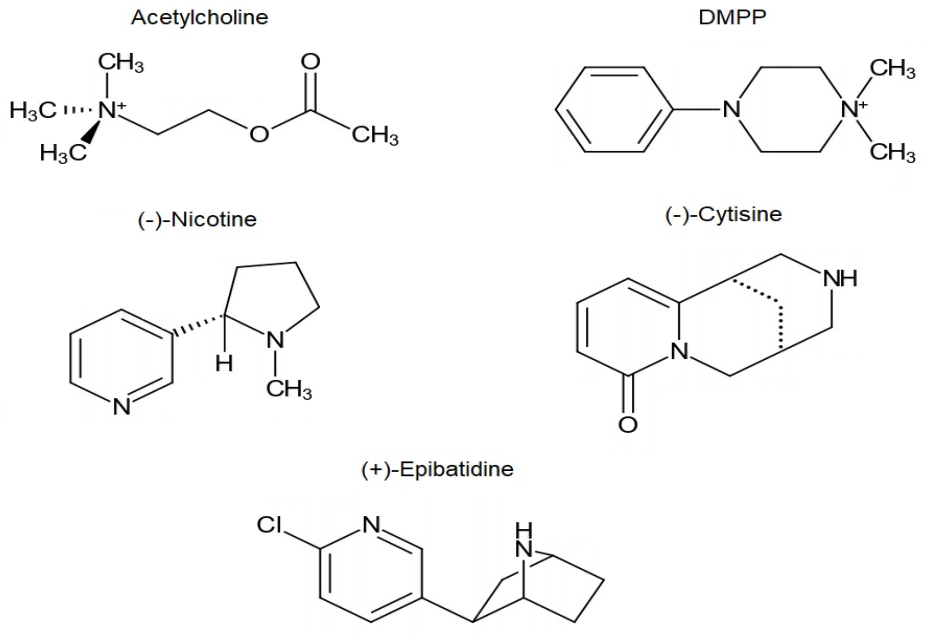

Figure 8 - Chemical structures of the most prominent agonists of nAChRs

The probably most famous exogenous agonist and name giver of nAChRs is nicotine ((1-Methyl 2-(3-pyridyl) pyrrolidine). This small alkaloid molecule can be isolated from the tobacco plant *Nicotiana tabacum* and is the major component of tobacco smoke leading to addiction and strong withdrawal effects and can alter nAChR regulated brain areas connected to sensory transmission, learning and memory, emotion, and the reward system (Brunzell *et al.*, 2015). The neurotoxic role of nicotine is profoundly studied, but there are also opposite findings that outline the neuroprotective properties of the molecule (Ferrea and Winterer, 2009).

Epibatidine (exo-2-(6-chloro-3-pyridyl)-7-azabicyclo-[2.2.1]heptane) an alkaloid isolated from the poison frog *Epipedobates tricolor* as part of one of the most potent nAChR agonists also gained a huge amount of attention because of its promising role in drug development. It was found that the analgesic potency of epibatidine is about 30 times higher than of nicotine (Salehi *et al.*, 2018) and 200 times higher than morphine (Traynor, 1998). But due to its high toxicity it was excluded as a therapeutic drug. Nevertheless, it is now broadly used to study the pharmacology of nAChRs experimentally, not only in the current work.

2.1.7 Antagonists of nAChRs

Antagonists of nAChRs have gained a lot of attention in the last decades. Due to their interaction properties with nAChR it was possible to investigate the receptors pharmacology in depth and as well to consider them in therapeutic treatments. They can be classified into two general groups, the competitive antagonists (CA) and the non-competitive agonists (NCA) (Pleuvry, 2004).

Some of the most investigated CA´s of nAChRs are e.g. α-bungarotoxin and α-conotoxins.
α-bungarotoxin can be isolated from the venom from the Southeast Asian banded krait, *Bungarus multicinctus* and is a 74 amino acid long neurotoxin with high affinity for nAChRs. The antagonist selectively and irreversibly blocks ACh binding sites in receptors at the neuromuscular junction, inhibiting ion flow and causing paralysis and it can in addition also inhibit homo-oligomeric α_7 and α_8 receptors (Young *et al.*, 2003).
α-conotoxins from the venom of cone snails can target different forms of nAChRs of the CNS and the neuromuscular junction. The subunit selectivity of several α-conotoxins has been the key to the characterization of native nAChR isoforms involved in modulation of neurotransmitter release, the pathophysiology of Parkinson's disease and nociception (Azam and McIntosh, 2009).

NCAs on the other hand do not compete for the same binding sites like agonists. NCAs can bind to nAChRs at several distinct and specific binding sites depending on the conformational state (closed, open and desensitized) of the receptor. They stabilize the receptor in a non-conducting conformation, like the closed or desensitized state and thus diminish the agonist's potency or affinity. Another possible mechanism is the direct block of the aqueous channel pore and therefore the prevention of ion flow through the receptor (Lees *et al.*, 2004). Some inhibitors bind to more than one binding site and can therefore inhibit receptor function in more than one mechanism.

Examples of NCAs are mecamylamine, an antagonist specific to neuronal nicotinic receptor subunits (Martin *et al.*, 1989) and barbiturates, which act as allosteric inhibitors of muscle-type nAChRs with high affinity for the open channel state (Hamouda *et al.*, 2014).

The coronaridine congeners 18-MC and (+)-catharanthine which act as NCAs of nAChRs are found to bind the receptors at the luminal, non-luminal and intersubunit sites. These two compounds are both part of this study and will be discussed in detail later.

2.1.8 nAChRs in heterologous expression systems

The structural and functional profile of nAChRs as well as their subunit composition have been investigated in different heterologous expression systems like e.g. Xenopus laevis oocytes, HEK293 cells or neuroblastoma cell lines over the past decades (Nelson and Lindstrom, 1999; Nelson *et al.*, 2001).

Many disadvantages of investigating nAChRs in heterologous systems have been pointed out by different studies showing that they might have effects on the properties of the receptor which then lead to conflicting observations. The absence of chaperons, the amount of mRNA used for the transfection, the different temperatures that are required when working with different expression systems like oocytes, diversities of N-glycosylation and intracellular signalling molecules that are involved in the receptor assembling process are all influencing factors worth mentioning (Lewis *et al.*, 1997; Millar, 2008; Nelson *et al.*, 2003; Pollock *et al.*, 2009; Sivilotti *et al.*, 1997; Zwart and Vijverberg, 1998). nAChR assembly is a tightly regulated process, at one point also limited by cell-specific mRNA expression which leads to certain subunit compilations in vivo and could lead to complete different in a heterologous expression system (Millar and Gotti, 2009). Preliminary studies found that e.g. the α_7 receptor subunits in neurons only form homo-oligomeric receptors but when they are co-expressed with other subunits in host organisms they can co-assemble as well into hetero-oligomeric receptors (Khiroug *et al.*, 2002). Other studies revealed that recombinant $\alpha_3\beta_4$ subunits have channel properties depending on the heterologous systems they were expressed in and do not resemble the characteristics of native $\alpha_3\beta_4$ receptors (Sivilotti *et al.*, 1997).

Previous investigations into comparing potency ratios (PRs) of two nAChR agonists (cytisine/DMPP) found that depending on where $\alpha_3\beta_4$ subunits are expressed the PRs change: m$\alpha_3\beta_4$ expressed in mouse SCG $\alpha_5\beta_2$ double KO PR 1.23, r$\alpha_3\beta_4$ expressed in HEK cells PR 1.47, h$\alpha_3\beta_4$ expressed in Xenopus oocytes PR 4.0 (David *et al.*, 2010). Different single channel properties of the same receptor type in different host organisms could also appear due to specific folding- and assembly behaviors or different post translational modifications (Lewis *et al.*, 1997). Since it is possible for $\alpha_3\beta_4$ receptors to either assemble in the 2(α_3)3(β_4) or 3(α_3)2(β_4) form, when transfected to host organisms the receptor favors the 3(α_3)2(β_4) form in HEK-cells and the 2(α_3)3(β_4) form in oocytes (Krashia *et al.*, 2010). To investigate the properties of different nAChRs in their native environment, primary SCG-neurons derived from KO mice with deletions of specific subunit genes were cultured and analysed (David *et al.*, 2010).

2.1.9 nAChR subunit composition in the native KO mouse SCG

In the past years several different nAChR KO mice have been generated, such as the β_2-KO (Picciotto *et al.*, 1995), the α_5-KO (Wang *et al.*, 2002) or the β_4-KO (Kedmi *et al.*, 2004). In additional double and triple KO animals were bred, which are viable and show surprisingly little phenotype. These knockout animals express unique receptor assemblies in the SCG (David *et al.*, 2010): Neurons in the SCG of a single β_2-KO contain about 75% $\alpha_3\beta_4$- and 25% $\alpha_3\beta_4\alpha_5$-receptors whereas a α_5-KO would leave 80% $\alpha_3\beta_4$- and 20% $\alpha_3\beta_4\beta_2$-assemblies. A double KO of α_5 and β_2 would thus lead to 100% of $\alpha_3\beta_4$ receptors in the mouse SCG (Figure 9). The α_5 and β_2 subunits are tightly regulated; when comparing WT with β_2 KO mice α_5 does not substitute for the loss of β_2 and vice versa, a KO of the α_5 gene does not affect the overall number of β_2 containing receptors. The β_2 subunit also cannot substitute for a KO of β_4. In the SCG of β_4-KO animals we find an overall reduction of the total receptors by about 85% (David *et al.*, 2010). KO experiments with mice SCGs nAChRs subunits, not only gave rise to the possibility of getting insight into the structural profile of different subunit- and receptor combinations in their natural environment, they as well allowed to illuminate their kinetic properties. Previous electrophysiological as well as biochemical approaches revealed the binding potencies of different agonists on individual nAChRs and their variable pharmacological behavior depending on subunit assembly, receptor distribution as well as the environment they are expressed in (David *et al.*, 2010).

Primary neurons cultured from the SCG of different wild-type and KO animals give the unique possibility to analyze defined nAChR-subunits in their native environment, and circumvent the difficulties of receptors expressed in heterologous expression systems (Ciuraszkiewicz *et al.*, 2013; David *et al.*, 2010).

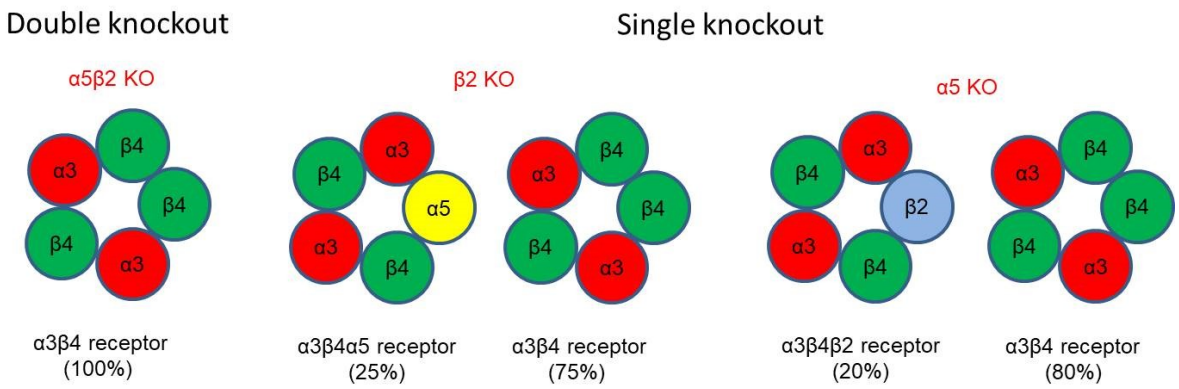

Figure 9 - Schematic representation of the receptors expressed in the SCG of WT mice after single or double KO of different subunit genes

A double KO of the α_5 and β_2 genes leads to a remaining 100 % of $\alpha_3\beta_4$-receptors. The single KOs showed distributions of 75% $\alpha_3\beta_4$- and 25% $\alpha_3\beta_4\alpha_5$-receptors for a β_2-KO and 80% $\alpha_3\beta_4$- and 20% $\alpha_3\beta_4\beta_2$-receptors for a α_5-KO.

2.2 Coronaridine congeners

Coronaridine congeners are either naturally occurring or synthetically produced indole alkaloids with known pharmacological properties such as for example psychoactive effects. They can be isolated from *Tabernanthe iboga*, a tree in West-Africa, belonging to the *Apocynaceae* family, and attracted interest in the fields of anti-addictive therapies. Out of a large group of iboga alkaloids one of the first identified members was ibogaine (Figure 10). Ibogaine was found to reduce drug dependence as well as withdrawal effects in humans such as for opiate, cocaine, alcohol and nicotine abuse for up to 6 months. Further studies showed that the substance as well decreases drug self-administration in rodents. However, ibogaine wasn't admitted as a therapeutic drug yet because of side effects like hallucinations, whole body tremors and damaged Purkinje cells in the Cerebellum (Antonio *et al.*, 2013; Arias *et al.*, 2017; Arias *et al.*, 2015). Other more promising relatives of the coronaridine family are 18-MC and (+)-catharanthine (Figure 11). 18-MC a synthetic iboga alkaloid congener also showed reduced drug self-administration in rats after administration but with fewer side effects. They all behave as NCAs of several nAChRs and where Ibogaine can affect different neurotransmitter systems simultaneously 18-MC and (+)-catharanthine have a much higher selectivity for specific nicotinic receptors (Glick *et al.*, 2000). Several previous studies outlined the anti-addictive properties of coronaridine congeners like 18-MC or (+)-catharanthine through their inhibitory mechanisms on $\alpha_3\beta_4$ nAChRs in the habenulo-interpeduncular cholinergic pathway (HICP) which modulates the dopaminergic brain reward

circuitry in the mesocorticolimbic system (Glick *et al.*, 2011; Maisonneuve and Glick, 2003; McCallum *et al.*, 2012).

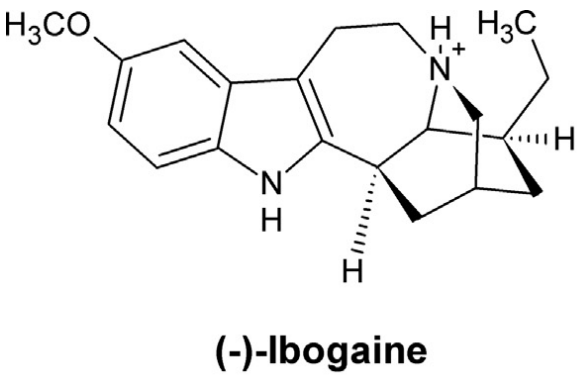

Figure 10 - Molecular structure of protonated (-)-Ibogaine

Adapted with permission from Dr. Hugo R. Arias (California Northstate University College of Medicine, Elk Grove, CA, USA) (Arias *et al.*, 2015).

Even though 18-MC and (+)–catharanthine are able to interact with different forms of the nAChR subunit compositions, the $\alpha_3\beta_4$ nAChRs gained huge attention because of their high expression levels in the HICP and in addition it could be proven that the congeners inhibit human $h\alpha_3\beta_4$ receptors with higher affinity than $h\alpha_4\beta_2$ receptors. The affinity of (+)–catharanthine for $h\alpha_3\beta_4$ was found to be about 18-fold higher than to $h\alpha_4\beta_2$ (Arias *et al.*, 2017; Arias *et al.*, 2010).

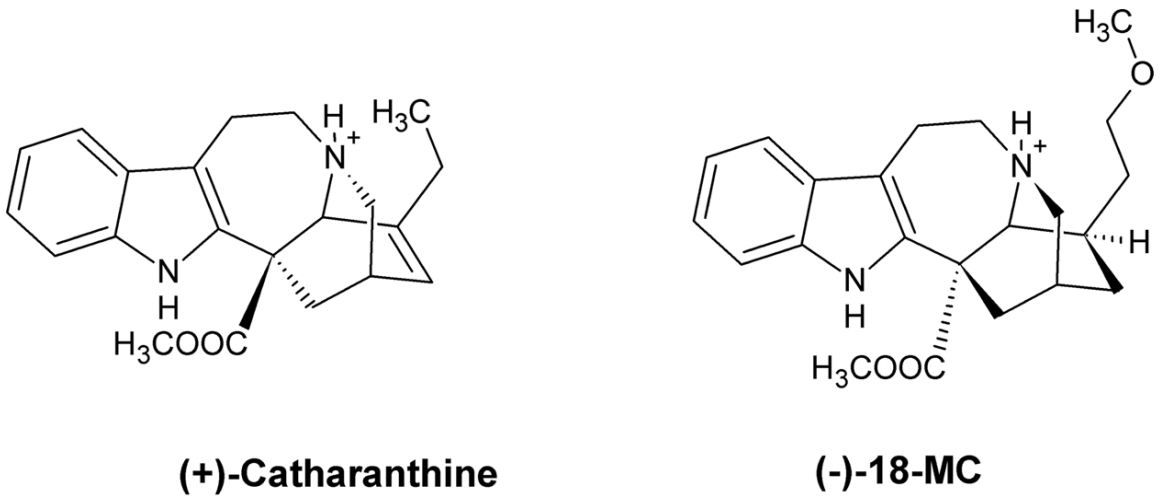

Figure 11 - Molecular structure of (+)-catharanthine and (-)-18-MC in their protonated state

Adapted with permission from Dr. Hugo R. Arias (California Northstate University College of Medicine, Elk Grove, CA, USA) (Arias *et al.*, 2015).

Calcium influx experiments on $h\alpha_3\beta_4$ receptors transfected to HEK293 cells showed that (+-)-18-MC inhibits Ca^{2+} -influx evoked by (±)-epibatidine in a cooperative mechanism, which corroborates more than one binding site or different mechanisms of inhibition. Other findings elaborated with patch clamp recordings in the mouse medial habenula (MHb) suggest non-cooperative binding of (+)–catharanthine and 18-MC even though the two results cannot be compared directly due to different experimental approaches (Arias *et al.*, 2017).

(-)-18-MC and (+)–catharanthine bind $h\alpha_3\beta_4$ nAChRs at the luminal, the non-luminal and the different intersubunit sites mostly via van der Waals interactions (Figure 12). The luminal site (green) of the nAChRs is located in the middle and forms the ion channel of the receptor. The non-luminal binding site (orange) is located close to the cytoplasmic end of the α_3 and β_4 transmembrane domains where the congeners interact with nonpolar residues at M1, M2 and M3 but (+)–catharanthine only binds to this location if it is protonated. Binding of (-)-18-MC to the intersubunit sites (red) appears to be between the α_3 and β_4 transmembrane spanning domains as well linked to residues exposed to luminal and non-luminal environments. (+)–Catharanthine additionally binds the $\beta_4\beta_4$-intersubunit (magenta) which is found near the extracellular end of two neighboring β_4 transmembrane spanning domains. (Figure 12) (Arias *et al.*, 2015).

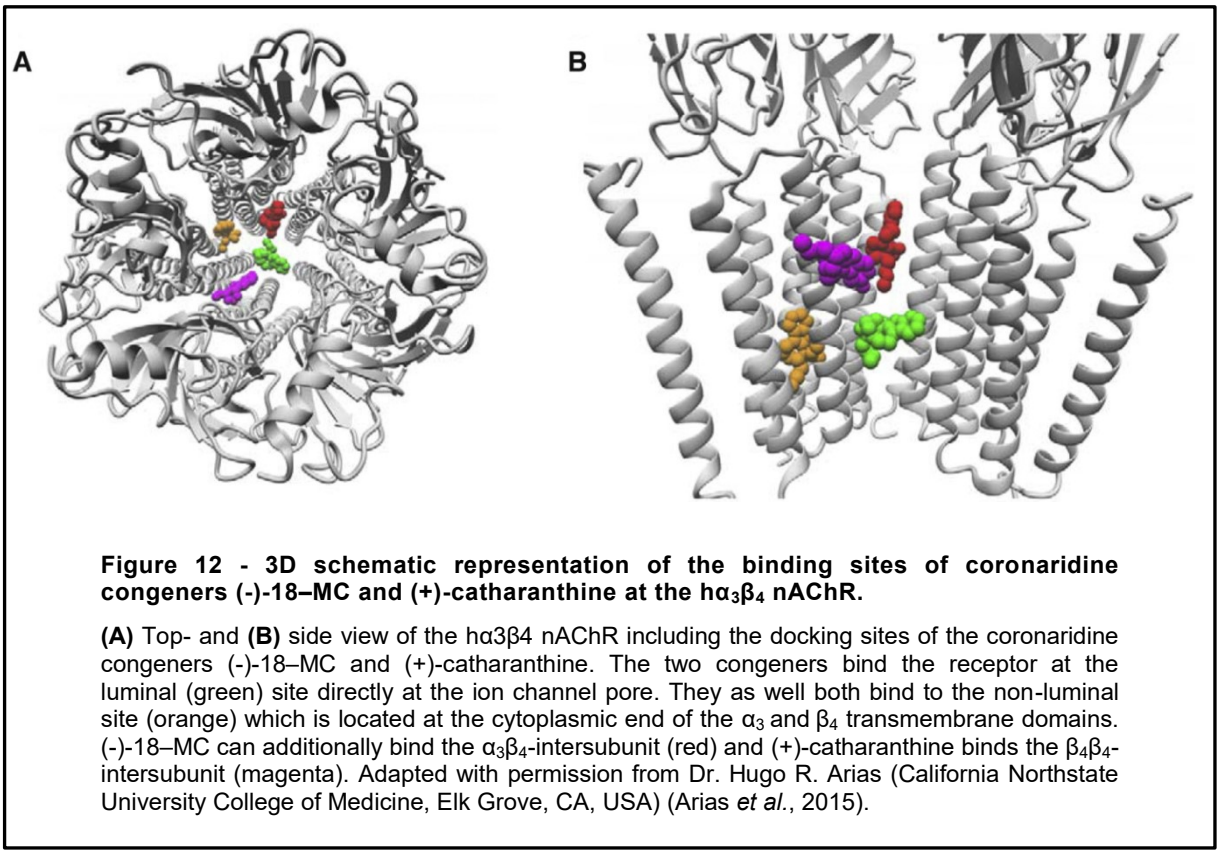

Figure 12 - 3D schematic representation of the binding sites of coronaridine congeners (-)-18–MC and (+)-catharanthine at the $h\alpha_3\beta_4$ nAChR.

(A) Top- and **(B)** side view of the hα3β4 nAChR including the docking sites of the coronaridine congeners (-)-18–MC and (+)-catharanthine. The two congeners bind the receptor at the luminal (green) site directly at the ion channel pore. They as well both bind to the non-luminal site (orange) which is located at the cytoplasmic end of the α_3 and β_4 transmembrane domains. (-)-18–MC can additionally bind the $\alpha_3\beta_4$-intersubunit (red) and (+)-catharanthine binds the $\beta_4\beta_4$-intersubunit (magenta). Adapted with permission from Dr. Hugo R. Arias (California Northstate University College of Medicine, Elk Grove, CA, USA) (Arias *et al.*, 2015).

The enantiomers of 18-MC, (+) - and (-)–18-MC are found to be equipotent at inhibiting $\alpha_3\beta_4$ nAChRs. The inhibition potency and interaction of 18–MC and (+)-catharanthine on nAChRs has been investigated over the past years using different heterologous model systems such as HEK293-h$\alpha_3\beta_4$ cells, TE671 cells, GH3-hα_7 subunit cells or mice brain slices MHb neurons, expressing α_3-containing nAChRs, including $\alpha_3\beta_4$, $\alpha_3\beta_2$, $\alpha_3\beta_4\beta_2$, $\alpha_3\beta_4\beta_3$, $\alpha_3\alpha_4\beta_4$, $\alpha_3\alpha_6\beta_4$, and $\alpha_3\alpha_5\beta_4\beta_2$ but they haven't been tested on specific nAChRs in their native environment yet (Arias *et al.*, 2017; Arias *et al.*, 2010; Arias *et al.*, 2015; Pace *et al.*, 2004).

2.3 Aims of this study

Preliminary studies have already revealed the interaction of many ibogaine relatives with nAChRs and highlighted the selectivity of 18-MC and (+)-catharanthine to α_3 - containing receptors especially the $\alpha_3\beta_4$-type, which is highly expressed in the HICP, an area strongly connected to the reward and addiction center in the brain.

These studies have yet only been made in heterologous expression systems that can strongly bias the natural behavior and kinetics of nAChRs and their interaction to agonists and antagonists. Fortunately, KO experiments in the mouse SCG allow isolating $\alpha_3\beta_4$-receptors (and others) in their natural environment which now makes it possible to investigate the two coronaridine congeners and estimate their behavior and inhibitory potency on the native mouse SCG nAChRs.

In this study I concentrated on the preparation of neurons from native mice SCG containing nAChRs with $\alpha_3\beta_2$, $\alpha_3\beta_4\alpha_5$ or $\alpha_3\beta_4\beta_2$ subunit assemblies in different specific stoichiometries depending on the WT or KO type. I measured the inhibitory potencies of 18-MC and (+)-catharanthine on (±)-epibatidine evoked whole cell currents in cell cultured neurons of the mouse SCG with perforated patch clamp whole cell recordings to characterize these antagonists interactions with distinct nAChR types.

3 Materials and methods

3.1 Animals

All experiments were performed with neurons from the SCG of mice pubs aged 4 to 5 (P-4, P-5) days from WT C57Bl/6J mice or mice carrying genetic deletions of the genes encoding the nAChR subunits α_5 (Wang *et al.*, 2002), β_2 (Picciotto *et al.*, 1995) or α_7 (Orr-Urtreger *et al.*, 1997). β_2 KO mice were generously provided by J.-P. Changeux (Pasteur Institute, Paris, France), and α_7 KO mice were purchased from Jackson Laboratories (Bar Harbor, ME, USA). Mice lacking both the α_5 and the β_2 subunits ($\alpha_5\beta_2$ double-KO) were obtained by crossing the two respective single-KO lines. The $\alpha_5\alpha_7\beta_2$ triple-KO mice were obtained by crossing $\alpha_5\beta_2$ double-KO mice with α_7 single-KO animals.
Animals were maintained at the local animal housing facility of the Medical University of Vienna and were fed standard chow and water *ad libitum.* They were housed with a light:dark regime of 12:12 h.

3.2 Preparation of neurons from mouse SCG

Standard reagents and materials: Carl-Roth, Merck, Sigma-Aldrich, Thermo Fisher-Scientific, Nunc

Calcium (Ca)-free Tyrode solution

NaCl	150 mM
KCl	4 mM
MgCl2.6H2O	2 mM
Glucose.H2O	10 mM
HEPES	10 mM
Aqua dest.	
Adjusted with NaOH to pH 7.4	

CD-Solution (Collagenase-Dispase in Ca-free Tyrode solution)

Collagenase IA (Sigma-Aldrich)	0.5 mg/mL
Dispase II (Sigma-Aldrich)	1 mg/mL
Ca-free Tyrode	Desired volume

Trypsin in Ca-free Tyrode solution

Trypsin (Worthington)	0.25 %
Ca-free Tyrode	

NMB++FCS

Gibco Neurobasal-A Medium (Fisher-Scientific)	
L-Glutamine (Sigma-Aldrich)	1.5 mM
Gibco-Penicillin-Streptomycin (10000 U/ml) (Fisher-Scientific)	10 µL/mL
Nerve growth factor NGF (R&D)	20 µg/L
Gibco B-27 Supplement (50x) (Fisher-Scientific)	20 µL/mL
Fetal calf serum FCS (Sigma-Aldrich)	10 %

Four to five day old (P-4, P-5) mice pubs were killed by decapitation with a sterile sharp scissor and the SCGs were dissected with sterile forceps and subsequently collected in ice-cold Tyrode. SCGs were carefully cleaned from tissue and blood vessels and transferred into a 5 mL tube with ice-cold Tyrode solution. The Tyrode was removed with a fire-polished Pasteur pipette and the SCGs were incubated in CD-solution for 20 min at 37 °C. After removal of the CD-solution the SCGs were washed once with Tyrode and incubated in 1 mL of Trypsin in Ca-free Tyrode-solution for 15 min at 37 °C. After removal of the Trypsin in Tyrode-solution the SCGs were incubated in prewarmed NBM++FCS for 2-3 min at 37 °C. Afterwards the NBM++FCS was removed and 0.5 mL of prewarmed NBM++FCS were added. The suspension was triturated with a fire polished Pasteur pipette by carefully pipetting up and down until the suspension was homogenous. The enzymes, trituration protocol and culture conditions were similar to published procedures (Fischer *et al.*, 2005), with the addition of 10% fetal calf serum (FCS, Sigma-Aldrich) to the culture medium during trituration.

The dissociated cells were seeded on poly-DL-lysine PDL (Sigma-Aldrich) + laminin (R&D Cultrex mouse laminin) coated petri-dishes (Nunc) and incubated with 1.5 mL B27-medium at 37 °C with 5 % CO_2 for later use.

3.3 Perforated patch clamp whole cell recordings

Standard reagents and materials: Carl-Roth, Merck, Sigma-Aldrich, Thermo Fisher-Scientific, Nunc.

Chemicals and Reagents

Amphotericin B (solid)	Sigma-Aldrich
(±)-epibatidine	Sigma-Aldrich
nAChR-antagonists:	
(+)-(+)-catharanthine (solid)	Gift from Dr. Hugo R. Arias (California Northstate University College of Medicine, Elk Grove, CA, USA)
18-MC (solid)	Gift from Dr. Hugo R. Arias

(+)-(+)-catharanthine was dissolved in DMSO for a 10 mM stock solution and stored at -20 °C. 18-MC was dissolved in ddH_2O for a 10 mM stock solution and stored at -20 °C. Desired concentrations were made from stock solutions by dilution with external buffer right before use.

Equipment

Borosilicate glass electrodes GB150-8P	Science Products GmbH
DAD-VM 12 valve drug application device	Adams & List
Axopatch 200B patch clamp amplifier	Axon Instruments
Digidata 1320A D/A converter	Axon Instruments

External buffer:

NaCl	120 mM
KCl	3 mM
MgCl2.6H2O	2 mM
Glucose	20 mM
HEPES	10 mM
CaCl2.2H2O	2 mM
Adjusted with 1 N NaOH to pH 7.3	

Internal buffer:

KCl	55 mM
K_2SO_4	75 mM
$MgCl_2$	8 mM
HEPES	10 mM
Adjusted with KOH to pH 7.3	

Electrophysiological recordings from mouse SCG neurons were performed at room temperature with perforated patch clamp technique (Rae *et al.*, 1991). The borosilicate glass electrodes had a tip resistance of 1.4 to 2.5 MΩ and were briefly front-filled with internal buffer and subsequently back-filled with internal buffer + 200µg/mL amphotericin B (final DMSO concentration: 0.8%).

The internal buffer + amphotericin B solution was freshly prepared every 60 minutes from a one-day stock solution (25 mg amphotericin B in 1 mL DMSO, 5min ultrasonic bath). Recordings were performed with cells kept for 3 to 4 days *in vitro*. It usually took about 3 to 8 minutes after establishing a gigaseal until the membrane capacitance indicated that an optimal access by the pore-forming antimycotic amphotericin B had been achieved. The cells were voltage clamped at -70mV.

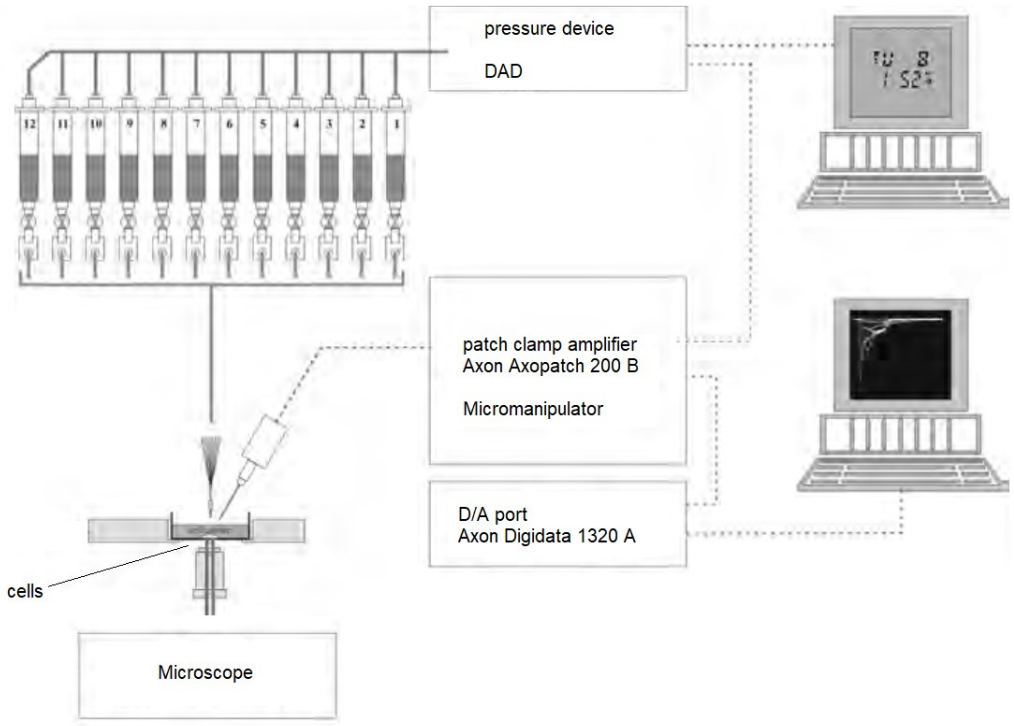

Figure 13 - Schematic representation of the drug application device (DAD) and the electrophysiological workstation Adapted from (Fischer, 2003).

All drugs were applied via the computer controlled DAD-VM 12 valve drug application device. This superfusion system delivers solutions from 12 reservoirs under adjustable pressure (220 mm Hg) via a quartz capillary with an inner diameter of ~100 µm and permits a complete exchange of solutions surrounding the cells (Figure 13).

To evoke whole cell currents, (±)-epibatidine (100 nM) was applied for 2 seconds on the patched cell. After 6 minutes a desired concentration of antagonist (x µM) was applied for 30 seconds directly followed by an application of (±)-epibatidine (100 nM) + antagonist (x µM) mixture for 2 seconds. After another 6 minutes (±)-epibatidine (100 nM) was once again applied for 2 seconds as a reference value. In between the drug application steps the cells were continuously superfused with external buffer to wash away agonists and antagonists. Before and after the application steps the cell capacitance (pF) was measured to monitor if the cells remained stable during the experiments. The DAD-VM drug application device was triggered over the patch clamp amplifier. For signal processing and recording of the whole cell currents an Axopatch 200 B patch clamp amplifier, a Digidata 1320A D/A converter and the pCLAMP 8 software (Axon Instruments) have been used.

3.4 Calculations

Inhibition by the two coronaridine congeners was determined by measuring the peak current induced by a submaximal concentration of (±)-epibatidine (100 nM) upon a 30 seconds pretreatment, and in the presence, of the antagonist (*Peak current II*, Figure 14 A). The peak current was then divided by the mean of the two peak currents (*Mean control current*, Equation A) measured in the absence of antagonist 6 minutes before (*Peak current I*, Agonist A) and 6 minutes after (*Peak current III*, Agonist B) the currents that were induced in the presence of the antagonist (Equation B). This regime was necessary because of the rundown of currents upon repeated applications of the agonist (Figure 14 B).

The interpolated *Mean control current* has been calculated by **Equation A**:

Equation A

$$Mean\ control\ current\ [pA] = \frac{Peak\ current\ I\ (Agonist\ A)\ [pA] + Peak\ current\ III\ (Agonist\ B)\ [pA]}{2}$$

Inhibitory effects of the antagonists were calculated as the percentage of the *Mean control current* in the absence of antagonists using **Equation B**:

Equation B

$$Peak\ current\ \% = \frac{100}{Mean\ control\ current\ [pA]} \times Peak\ current\ II\ [pA]$$

Half maximal inhibitor concentrations (IC_{50}) and Hill Slopes (nH) were calculated by non-linear regression with **Equation C** using Graphpad Prism 7:

Equation C

$$Y = \frac{100}{1 + 10^{((LOG\ IC50 - X) * HillSlope))}}$$

where x is the concentration of the inhibitor, and y the corresponding effect (in % of inhibition indicated as *Peak current %* in Equation B).

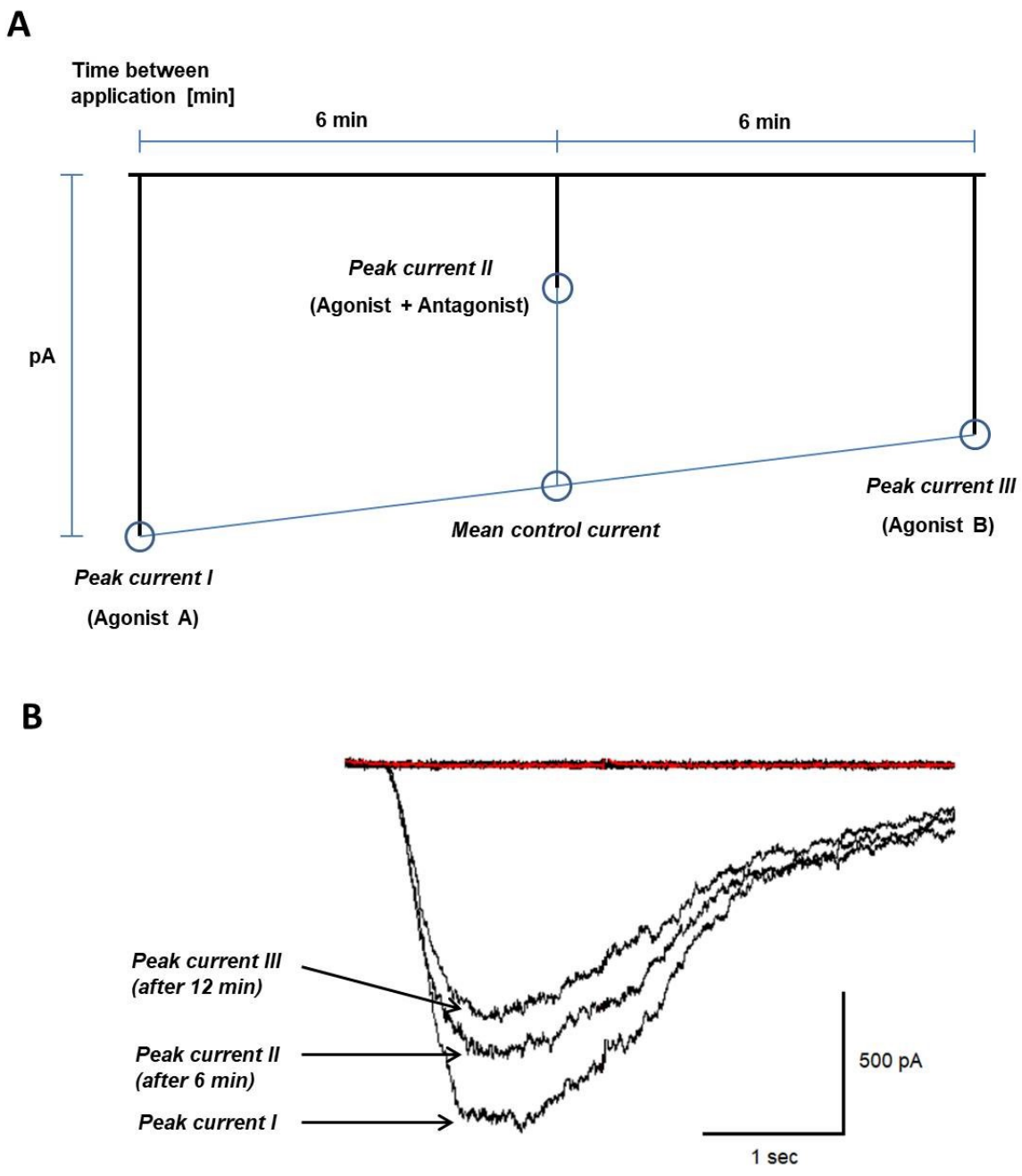

Figure 14 - Scheme for the calculation of the inhibitory effects of the antagonists

(A) Scheme for the calculation of the inhibitory effects of antagonists (+)-catharanthine and 18-MC indicated as *Peak current II*. Time between application (min) indicates the steps between the application of a submaximal concentration of (±)-epibatidine (100 nM) at the beginning (*Peak current I*), after 6 min (±)-epibatidine + antagonist (*Peak current II*) and after another 6 min (*Peak current III*). The calculation of the interpolated *Mean control current* (Equation A) was necessary to further calculate the inhibition (*peak current %,* Equation B). **(B)** Example of the rundown of whole cell currents upon repeated applications of 100 nM (±)-epibatidine on neurons of the WT mouse without antagonist. Currents have been measured at 3 different points with a 2 sec application of (±)-epibatidine, in the beginning (*Peak current I*), after 6 minutes (*Peak current II*) and after 12 minutes (*Peak current III*).

4 Results

4.1 Preparation of neuronal cell culture from newborn mouse SCG

I used cell cultures prepared from newborn WT (control) C57Bl/6J mice and from mice lacking the subunits β_2, α_5, α_7, or $\alpha_5\alpha_7\beta_2$, Table 2 shows the hetero-oligomeric receptors to be expected in these KO´s (David *et al.*, 2010). Receptors made of – or containing the - α_7 subunit do not significantly contribute to currents in response of agonists in mouse SCG neurons (David *et al.*, 2010). Hence, observations obtained from α_7 KO mice were pooled with data from WT mice.

Table 2 - Distribution [%] of nAChR subunits in neurons of the native mouse SCG in KO or WT animals

KO - group	Remaining nAChR subunits [%]
α_5	80% $\alpha_3\beta_4$, 20% $\alpha_3\beta_4\beta_2$ and α_7
β_2	75% $\alpha_3\beta_4$ and 25% $\alpha_3\beta_4\alpha_5$ and α_7
$\alpha_5\alpha_7\beta_2$	100% $\alpha_3\beta_4$
α_7	55% $\alpha_3\beta_4$, 24% $\alpha_3\beta_4\alpha_5$ and 21% $\alpha_3\beta_4\beta_2$
WT	55% $\alpha_3\beta_4$, 24% $\alpha_3\beta_4\alpha_5$, 21% $\alpha_3\beta_4\beta_2$ and α_7

4.2 Dose-response curve of (±)-epibatidine in cells prepared from α_7 KO mice

Maximal responses by (±)-epibatidine at a concentration of 200 nM was obtained in cells of 2 different cell cultures taken from a_7 KO mice. A concentration-response curve with an EC_{50} of 57 ± 4.3 nM and a Hill Slope = 1.95 ± 0.21 was obtained by setting the maximal responses from four cells to 100%, and by fitting the data by non-linear regression with Equation D:

Equation D

$$Y = \frac{100}{1 + 10^{((LOG\ EC50 - X) * HillSlope))}}$$

where x is the (±)-epibatidine concentration and y the corresponding effect (in %) (Figure 15). All experiments aimed at probing the inhibition by 18-MC and (+)-catharanthine were thereafter performed with 100 nM (±)-epibatidine.

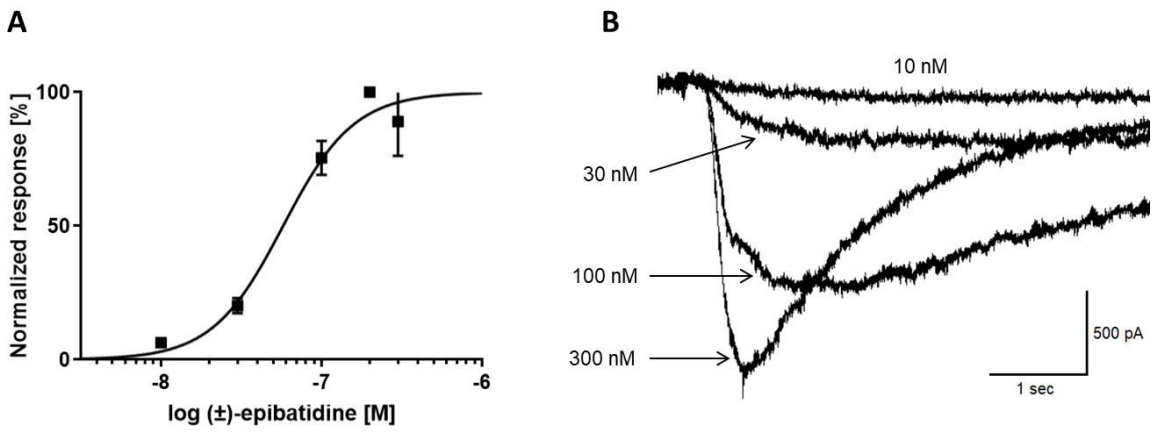

Figure 15 - Concentration response relationship for (±)-epibatidine in α_7 KO nAChR containing neurons of the mouse SCG

(A) Dose response curve for the activation of whole cell currents in α_7 KO nAChR containing neurons (n = 4 of two different preparations) of the mouse SCG with different concentrations of (±)-epibatidine (10, 30, 100, 200, 300 nM). (±)-epibatidine showed a *half maximal concentration* (EC_{50}) of 57 ± 4.3 nM (Hill Slope = 1.95 ± 0.21). **(B)** Whole cell currents of α_7 KO neurons after application of 10, 30, 100, 300 nM (±)-epibatidine for 5 sec.

4.3 Inhibition of (±)-epibatidine-evoked whole cell currents by the coronaridine congeners (+)-catharanthine and 18-MC

The inhibition of whole cell currents evoked by 100 nM (±)-epibatidine by the coronaridine congeners 18-MC and (+)-catharanthine was assessed as described in the methods (4.4).

SCG neurons were voltage-clamped at -70 mV and stimulated with 100 nM (±)-epibatidine for 2 sec at 3 measure points (*Peak current I, Peak current II and Peak current III*, Figure 14 A). Antagonists were applied 30 s before and during the 2 s stimulation with 100 nM (±)-epibatidine at *Peak current II*. Applications of antagonists alone did not produce any response. Figure 16 shows representative examples for the inhibition of (±)-epibatidine-evoked currents by 100 µM 18-MC or 100 µM (+)-catharanthine.

Both, 18-MC and (+)-catharanthine inhibition were rapid and reversible upon the 6 min washout of the antagonist with external buffer. *Peak current III* after 12 min evoked by 100 nM (±)-epibatidine was observed to be consistently smaller than *Peak current I*. This was assumed to be due to rundown effects of the whole cell currents upon repeated applications of 100 nM (±)-epibatidine as explained above (Figure 14 B).

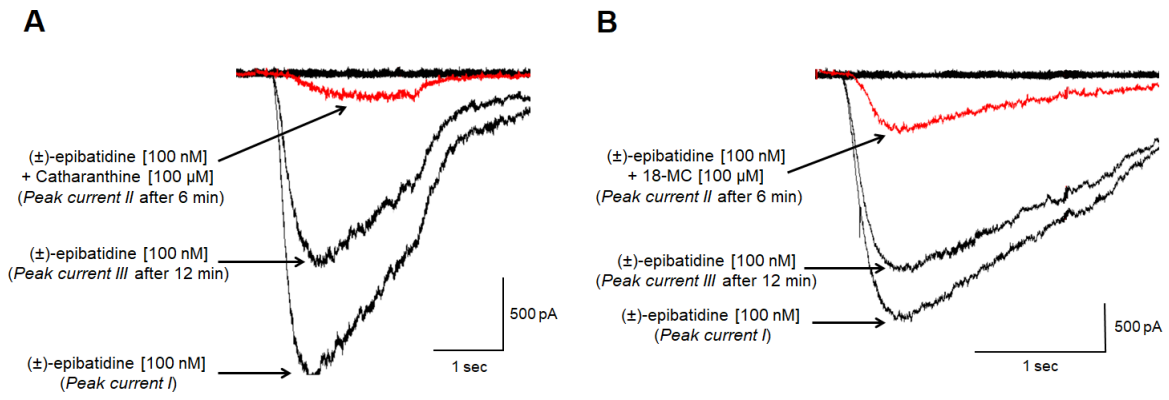

Figure 16 - Inhibition of (±)-epibatidine-evoked whole cell currents by the coronaridine congeners 18-MC or (+)-catharanthine

Rapid and reversible inhibition of (±)-epibatidine (100 nM) evoked whole cell currents by **(A)** 100 µM (+)-catharanthine in $\alpha_5\alpha_7\beta_2$ KO neurons or **(B)** 100 µM 18-MC in β_2 KO neurons indicated by red current lines. Three measurement points for each antagonist concentration measurement have been chosen to interpolate the corresponding inhibition potency of the respective antagonist: *Peak current I* evoked the largest current, *Peak current II* after 6 minutes of buffer washout was reduced by the corresponding antagonist concentration and *Peak current III* after 12 min was reduced due rundown effects (in this figure only the 100 µM (+)-catharanthine or 100 µM 18-MC concentrations are shown).

The curves in Figure 17 and Figure 18 show the concentration response relationship for the inhibition of (±)-epibatidine induced currents by (+)-catharanthine or 18-MC. IC_{50} values of the curves fitted to the data points with Equation C were used to compare the inhibition potencies of coronaridine congeners between the KO and WT neurons.

4.3.1 (+)-catharanthine

The inhibition of whole cell currents by (+)-catharanthine showed significant differences ($F_{1,27}$ = 16.3, $p < 0.01$) between the WT neurons with an IC_{50} of 30.0 ± 4.5 µM (IC_{50} + SE, n = 15 cells of 8 different preparations) and $\alpha_5\alpha_7\beta_2$ KO mice ($\alpha_3\beta_4$) with an IC_{50} of 12.2 ± 1.8 µM (IC_{50} + SE, n = 16 cells of 7 different preparations). (+)-catharanthine also showed a significantly higher inhibition potency on β_2 KO neurons with an IC_{50} of 8.9 ± 1.9 µM (IC_{50} + SE, n = 15 cells of 6 different preparations) compared to WT neurons ($F_{1,26}$ = 19.5, $p < 0.01$). Both, β_2 KO ($F_{1,29}$ = 11.29, $p < 0.01$) and $\alpha_5\alpha_7\beta_2$ KO ($F_{1,30}$ = 7.5, $p < 0.05$) inhibition by (+)-catharanthine was as well significantly different compared to the inhibition of α_5 KO-neurons. No significant differences have been found between the IC_{50} values for the inhibition of WT neurons compared to the α_5 KO-neurons with an IC_{50} of 23.0 ± 4.1 µM (IC_{50} + SE, n = 18 cells of 7 different preparations) or the $\alpha_5\alpha_7\beta_2$ KO- compared to β_2 KO neurons. The inhibitory potencies of (+)-catharanthine for the different KO animals followed the rank order β_2 KO >

$\alpha_5\alpha_7\beta_2$ KO > α_5 KO > WT. These results lead to the assumption that a KO of the β_2 subunit in β_2 KO and $\alpha_5\alpha_7\beta_2$ KO neurons may affect the binding properties of the nAChRs for (+)-catharanthine and that those neurons are most potently inhibited.

The Hill Slopes for the (+)-catharanthine inhibition are all higher than unity (-1) but lower than -0.5 which indicates either multiple binding sites of (+)-catharanthine on the different nAChRs or negative cooperative binding which causes that binding of one molecule of (+)-catharanthine decreases the affinity for other (+)-catharanthine molecules to the same receptor (Arias *et al.*, 2017; Copeland, 2013). Detailed information about the curve fitting parameters for the coronaridine congeners such as IC_{50} values, confidence interval (CI) and the goodness of fit (r^2) can be found in Table 3.

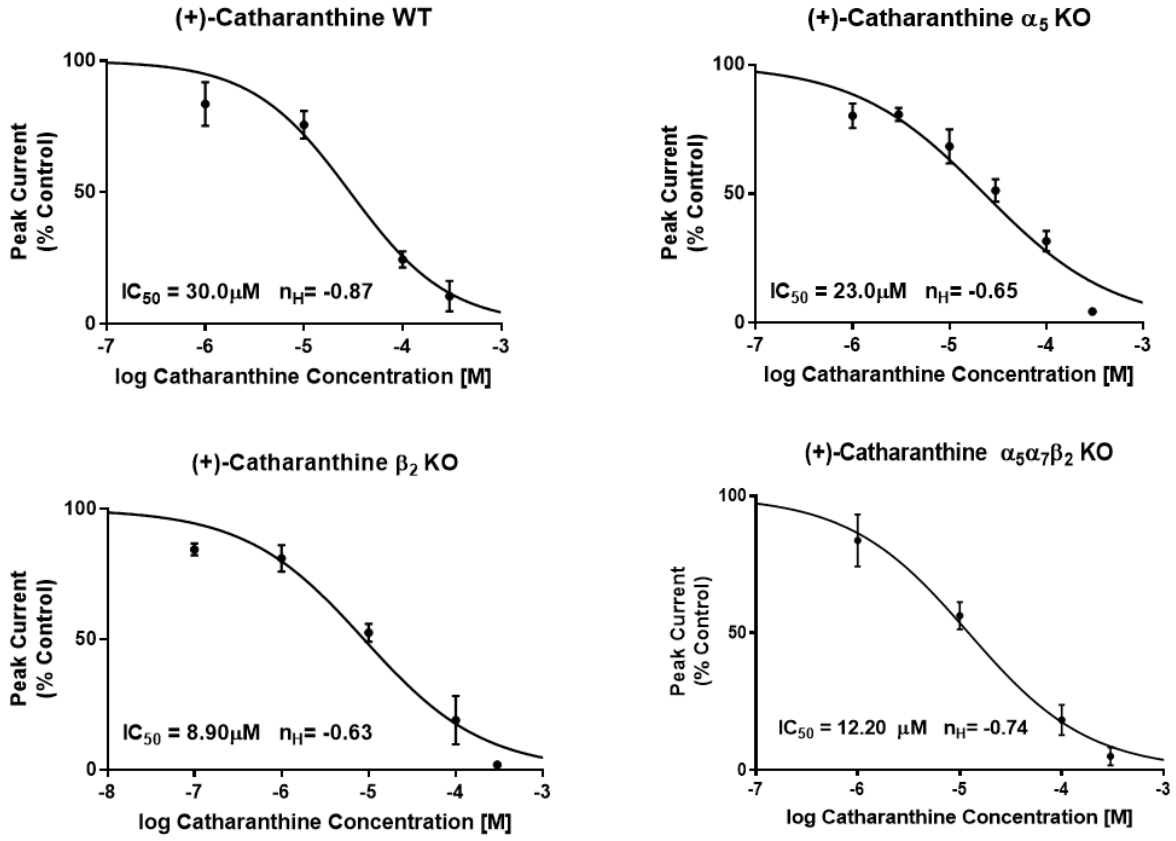

Figure 17 - Concentration response relationship for the inhibition of (±)-epibatidine-induced currents by (+)-catharanthine

The resulting inhibition-response curves are calculated as described above (4.4. Calculations). The response was normalized to the maximal (±)-epibatidine response (*Mean control current*, Figure 14) which was set to 100% here indicated as *Peak Current (% Control)*. The curves are plotted with their corresponding means and errors where the error bars represent the standard deviations (SD). Fit parameters are summarized in Table 3.

4.3.2 18-MC

The inhibition of whole cell currents by 18-MC did not show any significant differences between the KO- compared to the WT neurons. 18-MC inhibited WT or KO neurons with the following potencies: β_2 KO IC_{50} = 21.0 ± 6.1 µM (IC_{50} + SE, n = 12 cells of 5 different preparations), WT IC_{50} = 28.2 ± 11.2 µM (IC_{50} + SE, n = 25 cells of 13 different preparations), α_5 KO IC_{50} = 37.2 ± 15.0 µM (IC_{50} + SE, n = 13 cells of 6 different preparations) and $\alpha_5\alpha_7\beta_2$ KO IC_{50} = 93.0 ± 15.0 µM (IC_{50} + SE, n = 21 cells of 9 different preparations). The data of the curve-fitting calculations for 18-MC including KO-groups, IC_{50}, Hill Slopes, Goodness of fit parameters and the significant differences are summarized in Table 3.

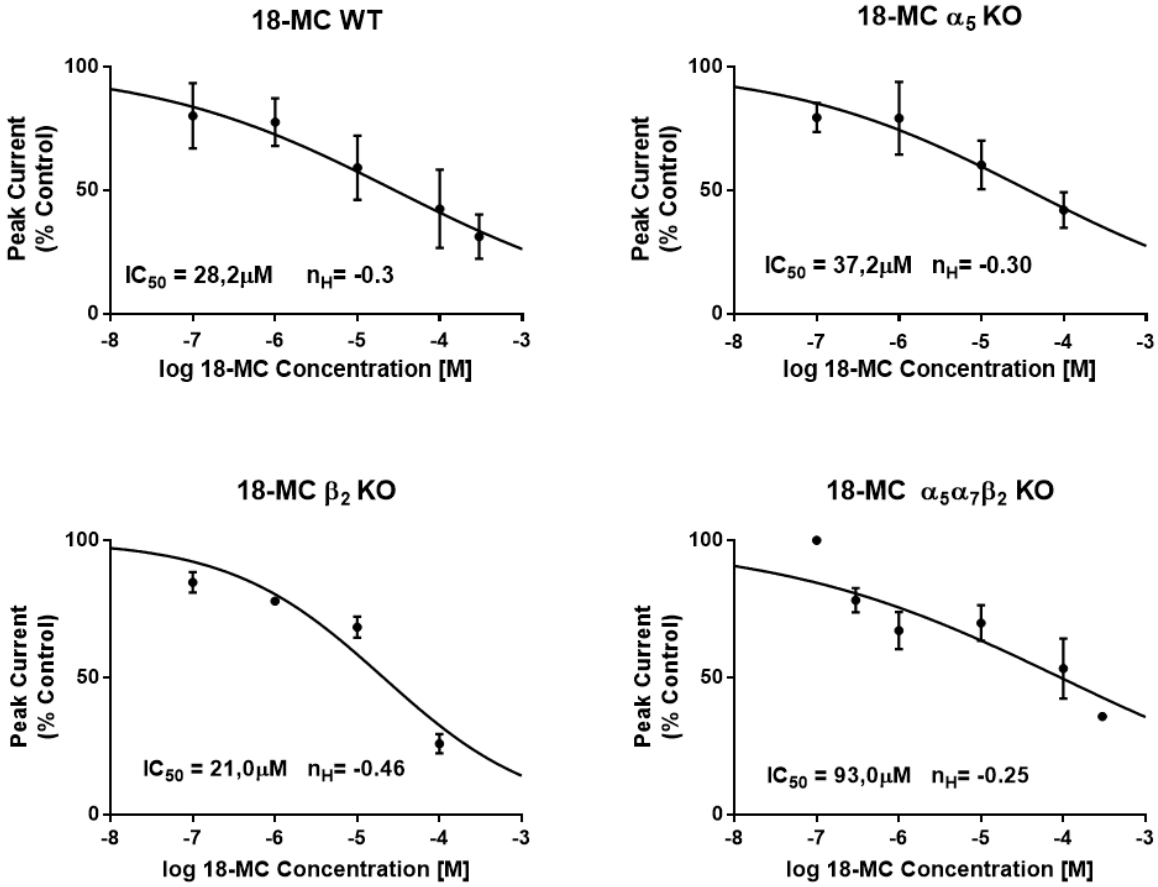

Figure 18 - Concentration response relationship for the inhibition of (±)-epibatidine-induced currents by 18-MC

The resulting inhibition-response curves are calculated as described above (4.4. Calculations). The response was normalized to the maximal (±)-epibatidine response (*Mean control current*, Figure 14) which was set to 100% here indicated as *Peak Current (% Control)*. The curves are plotted with their corresponding means and errors where the error bars represent the standard deviations (SD). Curve fitting and a statistical comparison of the 18-MC inhibition on the different nAChRs in WT and KO animals showed no significant differences between the distinct groups. The low Hill Slopes are assumed to be due to different reasons like binding of 18-MC to more than one binding site of the nAChRs, interaction of 18-MC to different possible receptor subunit arrangements and the poor water solubility of 18-MC at higher concentrations.

Interestingly 18-MC showed a relatively high IC_{50} on the $\alpha_5\alpha_7\beta_2$ KO- (93.0 µM, n_H = -0.25) compared to the other KO and WT neurons, nevertheless, statistically testing showed no significant differences between them. This could have several different reasons. The Hill slopes for the 18-MC inhibition are all higher than unity (-1) and as well higher than -0.5 indicating multiple binding sites of 18-MC on the different nAChRs or negative cooperative binding (Arias *et al.*, 2017; Copeland, 2013). Connected to this would be a possible biphasic binding behavior of 18-MC displaying a high- and low-affinity binding interaction with nAChRs caused by the multiple binding sites (Copeland, 2013) which would explain a poor curve fitting with Equation C. It as well turned out that 18-MC shows poor water solubility at higher concentrations which was indicated by a precipitation of 18-MC in the *External buffer* after preparation of a 300 µM antagonist solution, which in turn could be a reason for the flattened curve, the low Hill Slopes and the limited inhibition at concentrations above 100 µM.

Statistical comparison of the IC_{50} values in WT neurons showed no significant differences between (+)-catharanthine (IC_{50} of 30.0 ± 4.5 µM) and 18-MC (IC_{50} = 28.2 ± 11.2 µM). There were as well no significant differences found in α_5 KO neurons comparing the IC_{50} values of the two antagonists. Differences have been found between the β_2 KO- ($F_{1,23}$ = 5.9, $p < 0.05$) and the $\alpha_5\alpha_7\beta_2$ KO neurons ($F_{1,33}$ = 23.6, $p < 0.01$). But due to the poor curve fitting quality of the 18-MC inhibition this comparison must be viewed very critically.

Table 3 –Curve fitting parameters for the inhibition of (±)-epibatidine-evoked whole cell currents by the coronaridine congeners 18-MC and (+)-catharanthine

Coronaridine congener	Geno-types	IC_{50} ± SE [µM]	95% CI [µM]	Hill-Slope (n_H)	Goodness of fit (r^2)	Number of cells n (prep.*)	Significant differences p-values (compared to)
(+)-catharanthine	**WT or α_7 KO**	30.0 ± 4.5	20.9 – 41.1	-0.87	0.95	15 (8)	β_2 $p < 0.01$; $\alpha_5\alpha_7\beta_2$-KO $p < 0.01$
	α_5 KO	23.0 ± 4.1	15.9 – 33.4	-0.65	0.92	18 (6)	β_2-KO $p < 0.01$; $\alpha_5\alpha_7\beta_2$-KO $p < 0.05$
	β_2 KO	8.9 ± 1.9	5.5 – 14.3	-0.63	0.95	15 (6)	
	$\alpha_5\alpha_7\beta_2$ KO	12.2 ± 1.8	8.7 – 16.7	-0.74	0.97	16 (7)	
18-MC	**WT or α_7 KO**	28.2 ± 11.2	12.2 – 64.8	-0.30	0.75	25 (13)	
	α_5 KO	37.2 ± 15.0	16.3 – 115.4	-0.30	0.78	13 (6)	
	β_2 KO	21.0 ± 6.1	11.2 – 41.9	-0.46	0.89	12 (5)	(+)-catharantine β_2-KO $p < 0.05$
	$\alpha_5\alpha_7\beta_2$ KO	93.0± 45.2	37.2 – 335.4	-0.25	0.70	21 (9)	(+)-catharantine $\alpha_5\alpha_7\beta_2$-KO $p < 0.01$

prep.* = number of preparations

5 Discussion

In this work I demonstrated that the coronaridine congeners (+)-catharanthine and 18-MC effectively inhibit (±)-epibatidine induced whole cell currents in neurons of the mouse SCG containing native nAChRs with different expected subunit arrangements ($\alpha_3\beta_4$, $\alpha_3\beta_4\alpha_5$ and $\alpha_3\beta_4\beta_2$) by using perforated patch clamp whole cell recordings. Since coronaridine congeners have so far only been tested in heterologous expression systems, which can strongly influence the kinetic profile of the receptors, the aim of this study was to estimate the interaction of the two antagonists with nAChRs in their natural environment, to get a better understanding about their properties as well as their therapeutic potential.

Both, (+)-catharanthine and 18-MC inhibited nAChRs of all the KO and WT neurons rapidly, reversible and with different potencies. The (±)-epibatidine evoked currents fully recovered from inhibition after washout of antagonist containing solution with *External buffer.* This effect was observed in all neurons. This leads to the assumption that (+)-catharanthine and 18-MC bind nAChRs in a reversible way, which had already been suspected by previous experiments with brain slices of the medial habenula (MHb) (Arias *et al.*, 2017).

My findings show that the inhibition potency of (+)-catharanthine on native $\alpha_3\beta_4$ (as found in neurons from the $\alpha_5\alpha_7\beta_2$ KO) is significantly different and about 8 fold higher than the potency of 18-MC ((+)-catharanthine 12.20 µM : 18-MC 93.0 µM). Previous studies with Ca^{2+} influx experiments in HEK293-h$\alpha_3\beta_4$ cells showed results where (+)-catharanthine (IC_{50} 0.68 µM) is two times as potent as 18-MC (IC_{50} 1.47 µM) (Arias *et al.*, 2015). Other findings with patch clamp recordings in brain slices of the MHb resulted in IC_{50} values of 27.0 µM for (+)-catharanthine and IC_{50} 28.0 µM for 18-MC (Arias *et al.*, 2017). Neurons of the MHb express a huge variety of α_3 subunit receptors including $\alpha_3\beta_4$, $\alpha_3\beta_2$, $\alpha_3\beta_4\beta_2$, $\alpha_3\beta_4\beta_3$, $\alpha_3\alpha_4\beta_4$, $\alpha_3\alpha_6\beta_4$, and $\alpha_3\alpha_5\beta_4\beta_2$ subunits as well as α_4 containing nAChRs including $\alpha_4\beta_4$, $\alpha_4\beta_2$, and $\alpha_4\beta_3\beta_2$ subunits which all contribute to the overall currents measured but the largest proportion of the current response at MHb neurons has been attributed to $\alpha_3\beta_4$ containing nAChRs (Grady *et al.*, 2009; Quick *et al.*, 1999; Scholze *et al.*, 2012). Even though the previous data cannot be directly compared with the results of the current work due to different methodological approaches, the deviation of the potencies of the two nAChR antagonists compared to each other in the different model systems is huge and justifies a validation of their interaction in native mouse SCG neurons.

As mentioned above, the different results could be due to a variety of reasons like the choice of the model system used (e.g. heterologous, native), the methodologically approach (e.g. electrophysiological, Ca^{2+} influx), the different stoichiometry variants of a specific subunit containing receptor that can appear in different expression systems (e.g. ratio 2(α_3)3(β_4) :

3(α_3)2(β_4)) (Krashia *et al.*, 2010), as well as the variety of different subunit assemblies in distinct tissues of the nervous system e.g. the MHb or the mouse SCG and many more.

Comparison of the potencies of the two antagonists within the WT animals (leaving a distribution of nAChRs 55% $\alpha_3\beta_4$, 24% $\alpha_3\beta_4\alpha_5$ and 21% $\alpha_3\beta_4\beta_2$) showed no significant difference with similar IC_{50} values, (+)-catharanthine 28.2 µM and 18-MC 30.0 µM but different Hill slopes, (+)-catharanthine n_H = -0.87, 18-MC n_H = -0.30. This difference in the Hill slope could suggest a higher cooperative binding of (+)-catharanthine to the nAChRs than for 18-MC and even though and because of the low Hill Slope values it is thought that both of them bind in a non-cooperative reversible way. Previous studies found contrary behavior of the two congeners regarding binding cooperativity. Where Ca^{2+} influx experiments in HEK293-h$\alpha_3\beta_4$ cells indicate that the inhibitory process is mediated by a cooperative mechanism (Arias *et al.*, 2015), other electrophysiological measurements of neurons in the MHb show as well that the interaction acts in a non-cooperative way (Arias *et al.*, 2017) which is as well supported by the results of this work. But due to the fact that there is a mixed population of nAChRs in the WT animals of the mice´s SCG ($\alpha_3\beta_4$, $\alpha_3\beta_4\alpha_5$ and $\alpha_3\beta_4\beta_2$) it is difficult to make a statement about the binding cooperativity in WT animals. It is rather possible that (+)-catharanthine does not distinguish that much between the different nAChR types and that's why the inhibition response curves in the different KO and WT animals are steeper and show similar affinities compared to the 18-MC binding properties. 18-MC seems to distinguish even more between the different nAChR subtypes with a high and a low affinity binding component which could be one explanation for the flat appearance of the inhibition response curves.

The different inhibition potencies in-between the antagonists and KO/WT animals of the nAChRs could be due to different reasons. (+)-catharanthine showed a stronger inhibition to nAChRs that do not contain the β_2 subunit such as $\alpha_3\beta_4$ and $\alpha_3\beta_4\alpha_5$ receptors (as found in β_2 KO IC_{50} 8.9 µM and $\alpha_5\alpha_7\beta_2$ KO IC_{50} 12.2 µM) than the β_2 subunit containing receptors (as expressed in WT or α_7 KO, IC_{50} 30 µM and α_5 KO, IC_{50} 23 µM). This leads to the assumption that the β_2 subunit influences the affinity of the receptor for (+)-catharanthine. Since (+)–catharanthine binds h$\alpha_3\beta_4$ nAChRs at the luminal and the $\beta_4\beta_4$-intersubunit sites as well as the non-luminal sites if (+)–catharanthine is protonated, another reason for the distinct interaction behavior could be the distribution of $\beta_4\beta_4$-intersubunit sites in nAChRs (Arias *et al.*, 2015). The WT neurons leave about 55% of $\alpha_3\beta_4$ receptors some of which contain the $\beta_4\beta_4$-intersubunit sites, whereas triple KO neurons ($\alpha_5\alpha_7\beta_2$ KO) leave 100% $\alpha_3\beta_4$ receptors, from which some have a $\beta_4\beta_4$, while others have an $\alpha_3\alpha_3$ intersubunit site. This would explain the difference between the WT and the triple KO ($\alpha_5\alpha_7\beta_2$ KO) group but not the interaction

with β_2 KO and α_5 KO´s, where the distribution of $\beta_4\beta_4$-intersubunits in $\alpha_3\beta_4$ receptors is approximately the same (β_2 KO ~75% $\alpha_3\beta_4$ receptors and α_5 KO ~80% $\alpha_3\beta_4$ receptors) (David *et al.*, 2010).
The interaction of (+)–catharanthine to the $\beta_4\beta_4$-intersubunit binding site is only possible in the 2(α_3)3(β_4) stoichiometry of the nAChR. Since the $\alpha_3\beta_4$ receptor subunits can as well be arranged in a 3(α_3)2(β_4) stoichiometry (Krashia *et al.*, 2010) the $\beta_4\beta_4$-intersubunit would no longer be available for agonist binding. Preliminary studies found that in the SCG of early postnatal mice the mRNA levels of α_3 subunits are about 2-fold higher than β_4 mRNA levels (β_4/α_3 ratio of 0.44 at P1) (Putz *et al.*, 2008) which leads to the assumption that the $\alpha_3\beta_4$ receptor could favor the 3(α_3)2(β_4) stoichiometry.

18-MC binding to the distinct nAChRs differs from (+)–catharanthine interactions. The 18-MC inhibition response curves are flat and show very low Hill Slopes indicating multiple binding sites and/or negative cooperativity. Another reason could be a partitioning of the antagonist into an inactive, less potent form at higher concentrations caused by aggregation or insolubility (Copeland, 2013). Since I experienced a precipitation of 18-MC at high concentrations, its insolubility in aqueous milieus could be the reason for the low Hill Slopes and flat fitting curves.
The results also suggest that 18-MC binding could be favored by receptors containing the β_2 and/or α_5 subunits since the inhibition potencies are all in a range of about 21.0 to 37.0 µM except for the triple KO group ($\alpha_5\alpha_7\beta_2$ KO, IC_{50} = 93.0 µM). Additionally the inhibition response data of 18-MC on triple KO neurons gives reason to suggest biphasic binding behavior which indicates that 18-MC binds the two different nAChR populations (3(α_3)2(β_4) and 2(α_3)3(β_4)) or a high and low affinity binding site on one of the nAChR species with different affinities (Copeland, 2013). (-)-18-MC binds human(h)$\alpha_3\beta_4$ nAChRs at the luminal (pore), the non-luminal and the h$\alpha_3\beta_4$-intersubunit sites (Arias *et al.*, 2015). Unlike (+)–catharanthine which binds the $\beta_4\beta_4$-intersubunits, the additional binding of 18-MC to the $\alpha_3\beta_4$-intersubunit sites might as well be a reason for the distinct inhibition potencies.

5.1 Summary and Outlook

In conclusion, the current study gathers an insight into the interaction of the coronaridine congeners (+)–catharanthine and 18-MC with different nAChRs, containing distinct subunit combinations, in neurons of the mice SCG.

I showed that (+)–catharanthine and 18-MC not only bind the receptors with diverse inhibition potencies compared to each other but also in between the different WT and KO subunit animals. The results also suggest that binding of the two antagonists is influenced by the accessory subunits α_5 and β_2 as well that the different stoichiometric species in which the $\alpha_3\beta_4$ can occur show distinct affinities to the coronaridine congeners.

To confirm the current results, future studies might address performing Ca^{2+} release experiments of nAChRs in mice SCG to show if the differences in binding cooperativity is experiment depending or caused by the properties of nAChRs in heterologous expression systems as well as to exclude and confirm the flat fitting curves and low Hill Slopes of the 18-MC inhibition.

6 References

Akaike A., Shimohama S., Misu Y. (2018). *Nicotinic Acetylcholine Receptor Signaling in Neuroprotection*. Singapore, 191.

Albuquerque E.X., Pereira E.F., Alkondon M., Rogers S.W. (2009). *Mammalian nicotinic acetylcholine receptors: from structure to function*. Physiol Rev, 89(1): 73-120.

Antonio T., Childers S.R., Rothman R.B., Dersch C.M., King C., Kuehne M., Bornmann W.G., Eshleman A.J., Janowsky A., Simon E.R., Reith M.E., Alper K. (2013). *Effect of Iboga alkaloids on micro-opioid receptor-coupled G protein activation*. PLoS One, 8(10): e77262.

Arias H.R. (2000). *Localization of agonist and competitive antagonist binding sites on nicotinic acetylcholine receptors*. Neurochem Int, 36(7): 595-645.

Arias H.R., Jin X., Feuerbach D., Drenan R.M. (2017). *Selectivity of coronaridine congeners at nicotinic acetylcholine receptors and inhibitory activity on mouse medial habenula*. Int J Biochem Cell Biol, 92: 202-209.

Arias H.R., Rosenberg A., Feuerbach D., Targowska-Duda K.M., Maciejewski R., Jozwiak K., Moaddel R., Glick S.D., Wainer I.W. (2010). *Interaction of 18-methoxycoronaridine with nicotinic acetylcholine receptors in different conformational states*. Biochim Biophys Acta, 1798(6): 1153-1163.

Arias H.R., Targowska-Duda K.M., Feuerbach D., Jozwiak K. (2015). *Coronaridine congeners inhibit human alpha3beta4 nicotinic acetylcholine receptors by interacting with luminal and non-luminal sites*. Int J Biochem Cell Biol, 65: 81-90.

Azam L., McIntosh J.M. (2009). *Alpha-conotoxins as pharmacological probes of nicotinic acetylcholine receptors*. Acta Pharmacol Sin, 30(6): 771-783.

Beiranvand F., Zlabinger C., Orr-Urtreger A., Ristl R., Huck S., Scholze P. (2014). *Nicotinic acetylcholine receptors control acetylcholine and noradrenaline release in the rodent habenulo-interpeduncular complex*. Br J Pharmacol, 171(23): 5209-5224.

Borges L.S., Ferns M. (2001). *Agrin-induced phosphorylation of the acetylcholine receptor regulates cytoskeletal anchoring and clustering*. J Cell Biol, 153(1): 1-12.

Brunzell D.H., Stafford A.M., Dixon C.I. (2015). *Nicotinic receptor contributions to smoking: insights from human studies and animal models*. Curr Addict Rep, 2(1): 33-46.

Ciuraszkiewicz A., Schreibmayer W., Platzer D., Orr-Urtreger A., Scholze P., Huck S. (2013). *Single-channel properties of alpha3beta4, alpha3beta4alpha5 and alpha3beta4beta2*

nicotinic acetylcholine receptors in mice lacking specific nicotinic acetylcholine receptor subunits. J Physiol, 591(13): 3271-3288.

Copeland R.A. (2013). *Evaluation of Enzyme Inhibitors in Drug Discovery: A Guide for Medicinal Chemists and Pharmacologists*, John Wiley & Sons Inc, 572.

Corringer P.J., Le Novere N., Changeux J.P. (2000). *Nicotinic receptors at the amino acid level*. Annu Rev Pharmacol Toxicol, 40: 431-458.

Dani J.A. (2015). *Neuronal Nicotinic Acetylcholine Receptor Structure and Function and Response to Nicotine*. Int Rev Neurobiol, 124: 3-19.

Dani J.A., Bertrand D. (2007). *Nicotinic acetylcholine receptors and nicotinic cholinergic mechanisms of the central nervous system*. Annu Rev Pharmacol Toxicol, 47: 699-729.

David R., Ciuraszkiewicz A., Simeone X., Orr-Urtreger A., Papke R.L., McIntosh J.M., Huck S., Scholze P. (2010). *Biochemical and functional properties of distinct nicotinic acetylcholine receptors in the superior cervical ganglion of mice with targeted deletions of nAChR subunit genes*. Eur J Neurosci, 31(6): 978-993.

Dineley K.T., Pandya A.A., Yakel J.L. (2015). *Nicotinic ACh receptors as therapeutic targets in CNS disorders*. Trends Pharmacol Sci, 36(2): 96-108.

Fasoli F., Gotti C. (2015). *Structure of neuronal nicotinic receptors*. Curr Top Behav Neurosci, 23: 1-17.

Fenster C.P., Rains M.F., Noerager B., Quick M.W., Lester R.A. (1997). *Influence of subunit composition on desensitization of neuronal acetylcholine receptors at low concentrations of nicotine*. J Neurosci, 17(15): 5747-5759.

Ferrea S., Winterer G. (2009). *Neuroprotective and neurotoxic effects of nicotine*. Pharmacopsychiatry, 42(6): 255-265.

Fischer H. (2003). *Morphologic and Functional Characterisation of Somatic and Prejunctional Nicotinic Acetylcholine Receptor Channels in the Rodent Sympathetic Nervous System.* Faculty of natural sciences and mathematics University of Vienna. Doctor of science: 172.

Fischer H., Orr-Urtreger A., Role L.W., Huck S. (2005). *Selective deletion of the alpha5 subunit differentially affects somatic-dendritic versus axonally targeted nicotinic ACh receptors in mouse*. J Physiol, 563(Pt 1): 119-137.

Gahring L.C., Rogers S.W. (2006). *Neuronal nicotinic acetylcholine receptor expression and function on nonneuronal cells*. AAPS J, 7(4): E885-894.

Gerzanich V., Wang F., Kuryatov A., Lindstrom J. (1998). *alpha 5 Subunit alters desensitization, pharmacology, Ca++ permeability and Ca++ modulation of human neuronal alpha 3 nicotinic receptors*. J Pharmacol Exp Ther, 286(1): 311-320.

Glick S.D., Maisonneuve I.M., Szumlinski K.K. (2000). *18-Methoxycoronaridine (18-MC) and ibogaine: comparison of antiaddictive efficacy, toxicity, and mechanisms of action*. Ann N Y Acad Sci, 914: 369-386.

Glick S.D., Sell E.M., McCallum S.E., Maisonneuve I.M. (2011). *Brain regions mediating alpha3beta4 nicotinic antagonist effects of 18-MC on nicotine self-administration*. Eur J Pharmacol, 669(1-3): 71-75.

Gotti C., Clementi F., Fornari A., Gaimarri A., Guiducci S., Manfredi I., Moretti M., Pedrazzi P., Pucci L., Zoli M. (2009). *Structural and functional diversity of native brain neuronal nicotinic receptors*. Biochem Pharmacol, 78(7): 703-711.

Gotti C., Zoli M., Clementi F. (2006). *Brain nicotinic acetylcholine receptors: native subtypes and their relevance*. Trends Pharmacol Sci, 27(9): 482-491.

Grady S.R., Moretti M., Zoli M., Marks M.J., Zanardi A., Pucci L., Clementi F., Gotti C. (2009). *Rodent habenulo-interpeduncular pathway expresses a large variety of uncommon nAChR subtypes, but only the alpha3beta4* and alpha3beta3beta4* subtypes mediate acetylcholine release*. J Neurosci, 29(7): 2272-2282.

Graupner M., Gutkin B. (2009). *Modeling nicotinic neuromodulation from global functional and network levels to nAChR based mechanisms*. Acta Pharmacol Sin, 30(6): 681-693.

Hama A., Menzaghi F. (2001). *Antagonist of nicotinic acetylcholine receptors (nAChR) enhances formalin-induced nociception in rats: tonic role of nAChRs in the control of pain following injury*. Brain Res, 888(1): 102-106.

Hammond C. (2015). *Cellular and Molecular Neurophysiology*. San Diego, United States, Elsevier Science Publishing Co Inc, 444.

Hamouda A.K., Stewart D.S., Chiara D.C., Savechenkov P.Y., Bruzik K.S., Cohen J.B. (2014). *Identifying barbiturate binding sites in a nicotinic acetylcholine receptor with [3H]allyl m-trifluoromethyldiazirine mephobarbital, a photoreactive barbiturate*. Mol Pharmacol, 85(5): 735-746.

Harpsoe K., Ahring P.K., Christensen J.K., Jensen M.L., Peters D., Balle T. (2011). *Unraveling the high- and low-sensitivity agonist responses of nicotinic acetylcholine receptors*. J Neurosci, 31(30): 10759-10766.

Hogg R.C., Raggenbass M., Bertrand D. (2003). *Nicotinic acetylcholine receptors: from structure to brain function*. Rev Physiol Biochem Pharmacol, 147: 1-46.

Indurthi D.C., Lewis T.M., Ahring P.K., Balle T., Chebib M., Absalom N.L. (2016). *Ligand Binding at the 4-4 Agonist-Binding Site of the 42 nAChR Triggers Receptor Activation through a Pre-Activated Conformational State*. PLoS One, 11(8): e0161154.

Karlin A. (2009). 'Chapter 33: Nicotinic Acetylcholine Receptors'. Handbook of Cell Signaling. E.A.D. Ralph A. Bradshaw. San Diego, United States**:** 3048.

Kedmi M., Beaudet A.L., Orr-Urtreger A. (2004). *Mice lacking neuronal nicotinic acetylcholine receptor beta4-subunit and mice lacking both alpha5- and beta4-subunits are highly resistant to nicotine-induced seizures*. Physiol Genomics, 17(2): 221-229.

Keyser K.T., Britto L.R., Schoepfer R., Whiting P., Cooper J., Conroy W., Brozozowska-Prechtl A., Karten H.J., Lindstrom J. (1993). *Three subtypes of alpha-bungarotoxin-sensitive nicotinic acetylcholine receptors are expressed in chick retina*. J Neurosci, 13(2): 442-454.

Khiroug S.S., Harkness P.C., Lamb P.W., Sudweeks S.N., Khiroug L., Millar N.S., Yakel J.L. (2002). *Rat nicotinic ACh receptor alpha7 and beta2 subunits co-assemble to form functional heteromeric nicotinic receptor channels*. J Physiol, 540(Pt 2): 425-434.

Kracun S., Harkness P.C., Gibb A.J., Millar N.S. (2008). *Influence of the M3-M4 intracellular domain upon nicotinic acetylcholine receptor assembly, targeting and function*. Br J Pharmacol, 153(7): 1474-1484.

Krashia P., Moroni M., Broadbent S., Hofmann G., Kracun S., Beato M., Groot-Kormelink P.J., Sivilotti L.G. (2010). *Human alpha3beta4 neuronal nicotinic receptors show different stoichiometry if they are expressed in Xenopus oocytes or mammalian HEK293 cells*. PLoS One, 5(10): e13611.

Lees P., Cunningham F.M., Elliott J. (2004). *Principles of pharmacodynamics and their applications in veterinary pharmacology*. J Vet Pharmacol Ther, 27(6): 397-414.

Lewis T.M., Harkness P.C., Sivilotti L.G., Colquhoun D., Millar N.S. (1997). *The ion channel properties of a rat recombinant neuronal nicotinic receptor are dependent on the host cell type*. J Physiol, 505 (Pt 2): 299-306.

Lloyd G.K., Williams M. (2000). *Neuronal nicotinic acetylcholine receptors as novel drug targets*. J Pharmacol Exp Ther, 292(2): 461-467.

Maisonneuve I.M., Glick S.D. (2003). *Anti-addictive actions of an iboga alkaloid congener: a novel mechanism for a novel treatment*. Pharmacol Biochem Behav, 75(3): 607-618.

Martin B.R., Onaivi E.S., Martin T.J. (1989). *What is the nature of mecamylamine's antagonism of the central effects of nicotine?* Biochem Pharmacol, 38(20): 3391-3397.

McCallum S.E., Cowe M.A., Lewis S.W., Glick S.D. (2012). *alpha3beta4 nicotinic acetylcholine receptors in the medial habenula modulate the mesolimbic dopaminergic response to acute nicotine in vivo*. Neuropharmacology, 63(3): 434-440.

Millar N.S. (2008). *RIC-3: a nicotinic acetylcholine receptor chaperone*. Br J Pharmacol, 153 Suppl 1: S177-183.

Millar N.S., Gotti C. (2009). *Diversity of vertebrate nicotinic acetylcholine receptors*. Neuropharmacology, 56(1): 237-246.

Nelson M.E., Kuryatov A., Choi C.H., Zhou Y., Lindstrom J. (2003). *Alternate stoichiometries of alpha4beta2 nicotinic acetylcholine receptors*. Mol Pharmacol, 63(2): 332-341.

Nelson M.E., Lindstrom J. (1999). *Single channel properties of human alpha3 AChRs: impact of beta2, beta4 and alpha5 subunits*. J Physiol, 516 (Pt 3): 657-678.

Nelson M.E., Wang F., Kuryatov A., Choi C.H., Gerzanich V., Lindstrom J. (2001). *Functional properties of human nicotinic AChRs expressed by IMR-32 neuroblastoma cells resemble those of alpha3beta4 AChRs expressed in permanently transfected HEK cells*. J Gen Physiol, 118(5): 563-582.

Orr-Urtreger A., Goldner F.M., Saeki M., Lorenzo I., Goldberg L., De Biasi M., Dani J.A., Patrick J.W., Beaudet A.L. (1997). *Mice deficient in the alpha7 neuronal nicotinic acetylcholine receptor lack alpha-bungarotoxin binding sites and hippocampal fast nicotinic currents*. J Neurosci, 17(23): 9165-9171.

Pace C.J., Glick S.D., Maisonneuve I.M., He L.W., Jokiel P.A., Kuehne M.E., Fleck M.W. (2004). *Novel iboga alkaloid congeners block nicotinic receptors and reduce drug self-administration*. Eur J Pharmacol, 492(2-3): 159-167.

Picciotto M.R., Zoli M., Lena C., Bessis A., Lallemand Y., Le Novere N., Vincent P., Pich E.M., Brulet P., Changeux J.P. (1995). *Abnormal avoidance learning in mice lacking functional high-affinity nicotine receptor in the brain*. Nature, 374(6517): 65-67.

Pleuvry B.J. (2004). *Receptors, agonists and antagonists*. Neurosurgical Anaesthesia and Intensive Care, Pharmacology, 5(10): 350-352.

Pollock V.V., Pastoor T., Katnik C., Cuevas J., Wecker L. (2009). *Cyclic AMP-dependent protein kinase A and protein kinase C phosphorylate alpha4beta2 nicotinic receptor subunits at distinct stages of receptor formation and maturation*. Neuroscience, 158(4): 1311-1325.

Putz G., Kristufek D., Orr-Urtreger A., Changeux J.P., Huck S., Scholze P. (2008). *Nicotinic acetylcholine receptor-subunit mRNAs in the mouse superior cervical ganglion are regulated by development but not by deletion of distinct subunit genes*. J Neurosci Res, 86(5): 972-981.

Quick M.W., Ceballos R.M., Kasten M., McIntosh J.M., Lester R.A. (1999). *Alpha3beta4 subunit-containing nicotinic receptors dominate function in rat medial habenula neurons*. Neuropharmacology, 38(6): 769-783.

Rae J., Cooper K., Gates P., Watsky M. (1991). *Low access resistance perforated patch recordings using amphotericin B*. J Neurosci Methods, 37(1): 15-26.

Ramirez-Latorre J., Yu C.R., Qu X., Perin F., Karlin A., Role L. (1996). *Functional contributions of alpha5 subunit to neuronal acetylcholine receptor channels*. Nature, 380(6572): 347-351.

Rassadi S., Krishnaswamy A., Pie B., McConnell R., Jacob M.H., Cooper E. (2005). *A null mutation for the alpha3 nicotinic acetylcholine (ACh) receptor gene abolishes fast synaptic activity in sympathetic ganglia and reveals that ACh output from developing preganglionic terminals is regulated in an activity-dependent retrograde manner*. J Neurosci, 25(37): 8555-8566.

Salehi B., Sestito S., Rapposelli S., Peron G., Calina D., Sharifi-Rad M., Sharopov F., Martins N., Sharifi-Rad J. (2018). *Epibatidine: A Promising Natural Alkaloid in Health*. Biomolecules, 9(1).

Scholze P., Koth G., Orr-Urtreger A., Huck S. (2012). *Subunit composition of alpha5-containing nicotinic receptors in the rodent habenula*. J Neurochem, 121(4): 551-560.

Sivilotti L.G., McNeil D.K., Lewis T.M., Nassar M.A., Schoepfer R., Colquhoun D. (1997). *Recombinant nicotinic receptors, expressed in Xenopus oocytes, do not resemble native rat sympathetic ganglion receptors in single-channel behaviour*. J Physiol, 500 (Pt 1): 123-138.

Son C.D., Moss F.J., Cohen B.N., Lester H.A. (2009). *Nicotine normalizes intracellular subunit stoichiometry of nicotinic receptors carrying mutations linked to autosomal dominant nocturnal frontal lobe epilepsy*. Mol Pharmacol, 75(5): 1137-1148.

Tapia L., Kuryatov A., Lindstrom J. (2007). *Ca2+ permeability of the (alpha4)3(beta2)2 stoichiometry greatly exceeds that of (alpha4)2(beta2)3 human acetylcholine receptors*. Mol Pharmacol, 71(3): 769-776.

Traynor J.R. (1998). *Epibatidine and pain*. Br J Anaesth, 81(1): 69-76.

Wang H., Yu M., Ochani M., Amella C.A., Tanovic M., Susarla S., Li J.H., Wang H., Yang H., Ulloa L., Al-Abed Y., Czura C.J., Tracey K.J. (2003). *Nicotinic acetylcholine receptor alpha7 subunit is an essential regulator of inflammation*. Nature, 421(6921): 384-388.

Wang N., Orr-Urtreger A., Chapman J., Rabinowitz R., Nachman R., Korczyn A.D. (2002). *Autonomic function in mice lacking alpha5 neuronal nicotinic acetylcholine receptor subunit*. J Physiol, 542(Pt 2): 347-354.

Wilens T.E., Decker M.W. (2007). *Neuronal nicotinic receptor agonists for the treatment of attention-deficit/hyperactivity disorder: focus on cognition*. Biochem Pharmacol, 74(8): 1212-1223.

Xu W., Gelber S., Orr-Urtreger A., Armstrong D., Lewis R.A., Ou C.N., Patrick J., Role L., De Biasi M., Beaudet A.L. (1999). *Megacystis, mydriasis, and ion channel defect in mice lacking the alpha3 neuronal nicotinic acetylcholine receptor*. Proc Natl Acad Sci U S A, 96(10): 5746-5751.

Yost C.S., Winegar B.D. (1997). *Potency of agonists and competitive antagonists on adult- and fetal-type nicotinic acetylcholine receptors*. Cell Mol Neurobiol, 17(1): 35-50.

Young H.S., Herbette L.G., Skita V. (2003). *Alpha-bungarotoxin binding to acetylcholine receptor membranes studied by low angle X-ray diffraction*. Biophys J, 85(2): 943-953.

Zwart R., Vijverberg H.P. (1998). *Four pharmacologically distinct subtypes of alpha4beta2 nicotinic acetylcholine receptor expressed in Xenopus laevis oocytes*. Mol Pharmacol, 54(6): 1124-1131.

7 Appendix

7.1 List of Abbreviations

18-MC	18-methoxycoronaridine
Acetyl-CoA	Acetyl coenzyme A
ACh	Acetylcholine
AChE	Acetylcholinesterase
CA	Competitive antagonists
ChT	Choline transporter
CNS	Central nervous system
DAD	Drug application device
DMPP	3, 4-Dimethylpyrazole phosphate
EC_{50}	Half maximal effective concentration
HICP	Habenulo-interpeduncular cholinergic pathway
IC_{50}	Half maximal inhibitory concentration
IPn	Interpeduncular nucleus
KO	Knock out
mnAChR	Muscle type nicotinic acetylcholine receptors
nAChR	Nicotinic acetylcholine receptor
NCA	Non-competitive antagonists
PNS	Peripheral nervous system
PR	Potency ratio
SCG	Superior cervical ganglion
WT	Wild type

7.2 List of Figures

7.3 List of Tables

7.4 Zusammenfassung

Nikotinische Acetylcholinrezeptoren (nAChR) haben in den letzten Jahrzehnten aufgrund ihrer interaktiven Rolle im Belohnungssystem des Gehirns enorm an Aufmerksamkeit gewonnen. Dies gilt insbesondere für $\alpha_3\beta_4$ enthaltende Rezeptoren, die in Neuronen der medialen Habenula und des Nucleus interpeduncularis stark exprimiert sind und dort Entzugssymptome vermitteln.

Mehrere frühere Studien legten nahe, dass die beiden Coronaridin-Kongenere, (+)-Catharanthin und 18-Methoxycoronaridin vielversprechende neue Arzneimittelkandidaten sein könnten, da sie sich als nicht-kompetitive Modulatoren von $\alpha_3\beta_4$ exprimierenden nAChRs erweisen. Bis heute sind diese Verbindungen jedoch nur in heterologen Expressionssystemen untersucht worden. In der aktuellen Studie will ich nun die Interaktion der beiden Coronaridin-Kongenere mit nativen $\alpha_3\beta_4$ enthaltenden Rezeptoren in kultivierten primären Neuronen untersuchen.

Ich führte elektrophysiologische Messungen an kultivierten Neuronen des oberen Zervixganglions der Maus durch, welche unterschiedliche $\alpha_3\beta_4$ nAChR enthalten. Dafür wurden Knockout-Mäuse gezüchtet, welche nur bestimmte Untereinheiten des nikotinische Acetylcholinrezeptors exprimierten ($\alpha_3\beta_4$, $\alpha_3\beta_4\beta_2$ und $\alpha_3\beta_4\alpha_5$). Meine Ergebnisse zeigen, dass die beiden Kongenere die durch (±)-Epibatidin induzierten Ströme in den unterschiedlichen nAChR schnell und vollständig reversibel hemmen.

Die Unterschiede in den Hemmungspotenzen wurden nicht nur zwischen den beiden Kongeneren, sondern auch zwischen den durch die Kongenere gehemmten nAChR Subtypen, die in den unterschiedlichen Wildtyp- und Knockout-Neuronen exprimiert wurden, gefunden.

Die Ergebnisse deuten außerdem darauf hin, dass sich nikotinhaltige $\alpha_3\beta_4$ Rezeptoren in ihren Eigenschaften gegenüber den untersuchten Coronaridin-Kongeneren je nach Vorhandensein oder Fehlen der α_5 und β_2 Untereinheit unterscheiden.